Project ID: RLP 2002

Engineered 3D Microtissues for Personalized Cancer Treatment

A Major Qualifying Report submitted to the faculty of

WORCESTER POLYTECHNIC INSTITUTE

in partial fulfillment of the requirements for the degree of Bachelor of Science

This report represents the work of one or more undergraduate students submitted to the faculty as evidence of completion of a degree requirement. WPI routinely publishes these reports on the web without editorial or peer review.

Submitted by:

_____
Kylie Arnold (BME)

_____
Madeline Blake (BME)

_____
Marissa Gonzales (BME)

_____
Elena Raden (BME)

May 3, 2021

_____

Professor Raymond Page, Ph. D., Project Advisor

Department of Biomedical Engineering

Table of Contents

Authorship

All design, research, and experimentation components of this Major Qualifying Project were contributed to equally by all members of the team.

All sections of this report were written, edited, and formatted by all members of the team.

Acknowledgments

Our project was completed with the guidance and support of many WPI faculty and staff. We would like to thank the following individuals for their contributions to our project:

- Our advisor, **Professor Raymond Page**, for providing continuous guidance and advice throughout each stage of our project. We would also like to thank him for providing the stereo microscope and the HMF-52 fibroblast cell line.

- **Professor Sakthikumar Ambady** for providing the MDA-MB-231 GFP transfected cell line and for training us to use the fluorescent microscope.

- **Professor Marsha Rolle** for her advice on tissue ring formation techniques.

- **Dr. Erica Stultz** for her expertise and aid in 3D printing for our ring well punch.

- **Lisa Wall** for providing all our necessary lab needs and MQP lab access.

- **Worcester Polytechnic Institute** for the opportunity to complete a Biomedical Engineering Major Qualifying Project within the labs on campus.

Table of Figures

Table of Tables

Abstract

Recent developments in cancer research have shifted focus to personalized medicine to provide patients with individualized and effective cancer treatments. There is a lack of accurate *ex vivo* models that properly mimic tumor interactions and microenvironments. We have developed a protocol to create an *in vitro,* 3D, ring tumor model for use in cancer therapy testing. This model includes an agarose ring well, including a center post with a 2mm diameter at the base and a 2.5° inward taper, that was formed with a 3D printed punch that was designed using CAD. A mixed cell suspension of fibroblast cells (HMF-52) and GFP labeled breast cancer cells (MDA-MB-231) were incorporated into the ring models to represent tumor cells within healthy tissue. Fluorescence microscopy was utilized to observe cell distribution and behaviors within the rings after 4 days. Our design has shown evidence of microtumor integration within the ring, making the tissue ring setup a viable option for future tumor model development.

1.0 Introduction

Cancer is an indiscriminate health crisis that is the cause of 1 in 6 deaths worldwide [1]. In the United States, cancer is the second leading cause of death; annually, there are around 1.8 million diagnosed cases and about 600,000 deaths [2]. Despite the number of people affected, there is not a well-validated and effective method of treatment with high success rates for all patients. Treatment methodology is mainly dependent on the variety of cancer and the stage of cancer development. Cancer therapeutics have been rapidly evolving since its discovery in the late 1700s, beginning with surgical tumor removal in the mid 1800's, followed by chemotherapy, which has been in use since the 1930s [3]. Since then, other cancer therapies, such as radiation, immunotherapies, nano therapies, personalized medicine, and countless novel approaches, have developed within the last century.

Even with these advances, the standard treatments are not fully effective in numerous cancer cases. Following an initial therapeutic regimen, patients are often switched from one treatment method to another, or transitioned to combination methods with multiple treatment types [2]. A combination of treatments could be more effective in battling the cancer present, but it is difficult to determine which aspect is the most effective method in the path to remission. Another drawback of subsequent and combination treatments is that with the increase in rigor to try to treat the cancerous tissue, a grander toll is taken on the patient's healthy tissues and overall wellbeing. Particularly resistant or recurring cancer can further prolong and multiply the detrimental health effects of cancer treatment. Further stress on the body can arise from comingling of different medications and surgical techniques during the same timeframe.

Although prognoses are improving as research advances, the standard method of cancer therapy does not treat the majority of affected people appropriately and efficiently. To rectify this, there needs to be an improved way to screen, diagnose and treat cancer on a more individualized level. A personalized approach to cancer medicine would improve the effectiveness of initial treatment strategies. In recent years, personalized medicine research has escalated with help from 21st century data analytics, along with improved understanding of genomics and proteomics of both healthy and diseased states [4]. Personalized medicine incorporates medical history, environmental and health risks, genomics, proteomics and biomarkers to help predict the likelihood of developing cancer, diagnose cancer if it exists within the patient at that time, and effectively treat it once cancer forms. Personalized cancer treatment accounts for the patient's unique cancer and other factors in order to treat it in the most effective way and limit the negative effects on treatment to the rest of the patient's body.

While personalized medicine is a promising way to screen and treat cancer on an individual level, it is not a perfect system. Accuracy in utilizing biomarkers, proteins and other biological factors is limited by the databases these elements are compared to [4]. Personalized medicine is excellent for predicting and diagnosing cancer via these databases, but less effective at predicting the most effective regimen for a cancerous tumor *in vivo* because no two individuals' cancer are the same. These limitations emphasize the need for cancerous disease modeling and tissue engineering to treat cancer on an individual case-by-case basis [5].

One such concept to best treat cancer at an individual level is to isolate a person's cancerous cells, or take a biopsy of a solid tumor, and cultivate an *in vitro* model of a person's tumor. Once the tumor model is developed, countless drugs, medications, and a variety of other treatment methods can be tested for effectiveness. After identifying the most appropriate method with the best response against the cancer cells with minimal to no damage to surrounding healthy cells, the treatment can be applied to the patient. By first testing treatments *in vitro*, failed

treatment attempts on the patient are limited and combination therapy can potentially be avoided. As a step in this direction, we generated materials and methods to form contiguous tissue ring microtumor models. These initial 3D tissue models are the beginning stages of development of accurate *ex vivo* tumor models for use in patient specific cancer modeling and treatment testing.

The following paper and associated research aims to develop and validate an *in vitro* 3D ring tumor model for use in pre-clinical testing. To achieve this, we developed a tissue ring model that required the use of a 3D printed punch to create an agarose gel mold to then form tissue rings. The 3D printed punch and the agarose gel ring wells were the two major components necessary for our design. A positive punch was designed using SolidWorks 2020 software and 3D printed in rigid resin with glossy finish using an Objet 260 Connex printer. The punch is compatible for use with a standard 24-well plate. Metastatic breast cancer cells (MDA-MB-231) and normal breast fibroblast cells (HMF-52) were kept in culture and were suspended for use in the agarose gel ring wells. Two tissue ring types were created: a combination of HMF-52 cell suspension with an imbedded MDA-MB-231 spheroid and a co-culture suspension of the two cell types.

The tissue rings were evaluated to determine whether our methods formed replicable 3D tumor models, as well as an assessment of potential further research. The test protocols allowed cells to form self-aggregating 3D rings to represent a tumor microenvironment with surrounding healthy cells. These models were then monitored for replicability and for metastasis. This was accomplished through observations of migration and invasion. These observations and findings allowed us to determine if our model type and methods mimic *in vivo* tumor environment and enabled us to make recommendations for future research.

The contents of this paper include a thorough literature review in chapter 2 of current published works on similar topics. In this chapter, the team outlines that technological background and what has been previously tested and proved in our field. Chapter 3 the project strategy, explains the intended research milestones and our project objectives. In addition to this, the design requirements and constraints, along with a timeline of our research are outlined in this chapter. The design process is explained in chapter 4. The focus of this chapter is to present the reasonings behind the team's design decisions. This section also dives into the conceptual designs and potential prototypes for the final design. Chapter 5, the design process outlines the course of our experimentation. This chapter overviews our research methods, observations and results. Following this, chapter 6 discusses the final design components and methodology, in addition to design considerations and engineering impacts. Chapter 7, the discussion, analyzes the results from chapters 5 and 6 and overviews some of the limitations of our design and the research we completed. Finally, in chapter 8, the team summarizes the conclusions of our research and proposes recommendations for future work by other MQP teams.

2.0 Literature Review

This chapter outlines the physiological, methodological and technological background needed to guide decision making and progress throughout this project. This section specifically describes cancer, types of *ex vivo* cell modeling, and personalized medicine's potential impact on cancer treatment.

2.1. Cancer

Cancer is a blanket term for a range of conditions characterized by abnormally proliferating cells that spread to surrounding tissues [6]. Cancer cells can arise from any cells of the body, and the form of cancer is named based on where the cancer cells originated (example: breast) or the type of cells that are cancerous (example: connective tissue cells). Normal, healthy cells follow a regulated cell life cycle with controlled proliferation and programmed cell death. Cancer cells typically do not differentiate like healthy cells due to genetic mutations or environmental factors affecting gene expression and because of this, they do not follow a typical cell cycle. Cancerous cells proliferate rapidly and do not undergo apoptosis, which can result in tumors or widespread infiltration of cancer cells. Malignant tumors can invade surrounding healthy tissues and cause damage. Cancer cells can also spread through the blood and form tumors in other parts of the body. Cancer cells are able to alter surrounding cells, biomolecules and vasculature to benefit the growth and spread of the tumor. Cancer cells can also influence the immune system to prevent the immune system from breaking down the harmful cancer cells. The mechanisms that cause cancer to arise can be simplified into DNA mutations, through environmental factors such as UV radiation or through mistakes in typical DNA replication during cell division. Specific parts of the genome are typically considered drivers of cancer development. These include protooncogenes and tumor suppressor genes, which both control normal cell growth and division, as well as DNA repair mechanisms which are intended to fix genetic mistakes to prevent cancerous cell formation. Cancer that originates and grows in one part of the body then migrates and develops in a secondary location is considered metastatic.

2.1.1. Metastasis

The regional form of metastasis is when a part of a tumor or cancer cells in one part of the body breaks off and implants in another region of the body via the lymphatic system or blood vessels [7]. If a cancer metastasizes in this way, the type of cancer is still based on where the cancer originated. Cancer can metastasize locally and infect nearby cells and tissues. Steps of metastasis generally occur in this order: cancer invasion of nearby tissue, moving through tissue into blood or lymph vessels, traveling via bloodstream or lymphatic system to elsewhere in the body, moving out of the transport vessels into surrounding tissue, developing a secondary tumor in this tissue, and lastly alteration of the microenvironment in which new blood vessels form that supply the tumor with blood [8]. The cancer cells that leave the primary cancer site and can cause metastasis are called circulating tumor cells (CTCs). Different types of primary cancer tend to metastasize to a certain group of secondary regions. For example, breast cancer typically metastasizes to bone, brain, lung or liver tissue. It is important to understand the typical metastasis progression of cancer to track and predict the cancer path.

2.1.2. Circulating Tumor Cells

Circulating tumor cells (CTCs) are full of genetic information and mutations that originate from the main tumor and enter the lymphatic system and bloodstream and end up in areas of healthy tissue that they embed in and proliferate on [9]. CTCs not only travel as individual cells, but also as cell clusters known as circulating ensembles of tumor-associated cells (C-ETACs) [10]. CTCs carry a lot of information about the originating tumor, and this information can help researchers and medical professionals determine the best route to treat the cancer patient.

Cancer is traditionally diagnosed through very invasive methods of tumor tissue biopsies that undergo histologic examination (HPE). This method requires specialized imaging, and the whole process not only takes a physical toll on the patient, but also a financial toll [11]. Using CTCs and C-ETACs as cancer biomarkers only requires a blood sample from the patient. Due to there being a very small number of CTCs present in the blood in comparison to other cells (approximately 10 CTCs/mL), various methods have been developed to gain access to the CTCs in the blood [12]. One of the first methods was through size-based filtration. A blood sample is spun down into its layers, and the CTCs remain with the white blood cell layer. Because CTCs are larger than white blood cells, they can be pulled out with filtration. Another approach involves the antibodies against epithelial cell-adhesion molecule (EpCAM) that stick out on the surface of CTCs. These antibodies attach to magnetic beads, so when a magnetic field is applied, the CTCs can be removed [9]. There are also various microfluidics-based devices that, through a series of chambers and pathways, are able to pull CTCs from the blood.

The presence of CTCs in a cancer patient's blood can be very helpful in some metastatic cancers, like metastatic breast cancer. For breast cancer patients, it has been found that those with fewer CTCs present in their blood tend to live longer than those with more [9]. However, the methods for capturing CTCs have yet to reveal information for meaningful applications in the medical field past a numerical evaluation for prognostication. This is where C-ETACs become helpful. C-ETACs can be harvested from whole blood and further analyzed to tell more about the cancerous tumor that they come from. Peripheral blood mononuclear cells are first taken from whole blood and are then treated with epigenetically activating media. Phase contrast microscopy helps to determine C-ETACs and CTCs from the sample, and immunocytochemistry helps pull out only C-ETACs and characterize them through organ-specific and subtype-specific antigens [11]. This further analysis of C-ETACs makes this noninvasive cancer diagnosis comparable to HPE and has the potential to diagnose asymptomatic patients through a blood test.

2.1.3. Detection and Diagnosis

Early detection and diagnosis of metastatic cancer could greatly affect the outcome of early therapeutic treatments for patients. The issue, however, is that it can be extremely difficult to detect metastasis. Traditionally, technology used to detect cancer at the origin of the tumor cannot be used to detect metastatic cancer. For example, using a mammogram to detect breast cancer cannot be used for other areas of the body [13]. Current methods for detecting metastatic tumors include PET and CT scanning and biomarkers. PET and CT scans can have an increased accuracy by combing multiple approaches, but struggle to detect bone metastases or tumors below a certain size [14]. Biomarkers can track the spread of disease to other sites and can assist oncologists when deciding which treatment method would be most appropriate for patients with metastatic cancer [15]. While biomarkers can be extremely useful, imaging modalities still produce higher accuracy and sensitivity in detecting or predicting the propensity of metastatic

tumors [14]. As a result of these drawbacks, newer technologies and methods are needed for early detection of metastatic tumors. Monitoring CTCs in the peripheral blood could be used to show prognosis of various cancers and to predict metastasis [16]. While this approach may have serious potential, significant advances need to be made to improve the materials methodologies associated with monitoring CTCs. With these changes, monitoring CTCs could help improve and enhance early detection and diagnosis of metastasis in cancer patients.

2.1.4. General Treatment

Cancer treatment depends on type of cancer (type of cell and tissue of origin), stage of cancer progression, and what is determined to be most safe for the patient. There are 10 broad types of cancer treatment [17]. The first is surgery. If the cancer is localized and able to be isolated, a tumor can be surgically removed. Usually, surgery is followed by other forms of cancer therapy to be thorough in the treatment process. Chemotherapy for cancer is the use of powerful drugs that target and kill quickly dividing cells. Radiotherapy, either internal or external, utilizes high energy ionizing radiation to destroy the DNA of cancer cells in an area. A drawback of radiotherapy is that it damages healthy cells within the area because it does not differentiate between healthy and cancerous cells. Some patients require stem cell and bone marrow transplants in tandem with chemo- and radiotherapy to help the patient recover from the detrimental effects of these therapies. Cancer drugs are used to treat cancer itself and/or to relieve symptoms of cancer. Hormone therapy can be used to lower hormone levels within the body and subsequently slow or stop the proliferation of cancer cells. Immunotherapy works to help the patient's own immune system to seek out, recognize and attack cancer cells. Personalized medicine is individualized treatment based on multiple factors. Personalized medicine aims to use genetics and other individual identifiers to best eradicate the cancer cells while causing minimal damage to healthy tissues. In order to develop more effective cancer treatments, it is important to test various methods on models to determine efficacy of the treatment before applying it to patients. The different types of models that can be utilized in this research are detailed in the next sections.

2.2. 2D Cell Culture

One of the most basic methods to study cell behavior and interaction is by culturing cells on 2D surfaces. 2D cell cultures can be used to study some behaviors of cancer cells, but overall, 2D methods tend to oversimplify the environment and activity of cancer cells. This oversimplification results in differing gene profiles that are responsible for the cell invasion and migration, as well as angiogenesis [18]. The modulus of the plastic plate in which cells reside is much harder than any internal body tissue, which can cause increased cell adhesion to the surface. When this happens, cells may stretch and become flat, which will, in turn, change the cell phenotype and the behaviors exhibited by the cells [19]. These behaviors can include differentiation, proliferation, apoptosis, along with changes to the cell's DNA transcription and, thus, protein expression.

In addition to this, cells are grown on a monolayer and the only cell-cell connections formed are on the lateral edges of the cells. The top of the cells are exposed to the media and cells receive a homogenous amount of nutrients and growth factors while the bottom of the cells are interacting with the culture plate. Another issue of monolayers is that only living cells are attached and interacting with other cells. This is because when cells die in a 2D culture they

detach from the surface of the plate and float in the media. Contrary to this, *in vivo* necrotic cells may lead to further necrosis in otherwise healthy cells. For these reasons, 2D cell culture is ineffective for disease modeling and researchers are turning to 3D models to mimic the *in vivo* state.

2.3. 3D Cell Culture

3D cell culture allows for a more accurate depiction of the behavior of cells in a physiological environment. This section will discuss the various types of 3D models that can be used, as well as how they are created.

2.3.1. In vivo models

Animal models, and more specifically rodent models, have been an important aspect in cancer studies. Animal models allow for studies of tumor development and progression, as well as research into various cancer therapies, treatments and anticancer agents [18]. Due to having physiology that resembles that of humans, mice are used to study gene function and the molecular mechanisms of cancer *in vivo* [20]. Apart from the similar physiologies, mice are advantageous as *in vivo* cancer models because "(a) They are small in size; (b) they are inexpensive to maintain; (c) they reproduce rapidly and have large litters; and (d) they can be genetically manipulated" [20]. Mice are used in a variety of manners for cancer research. They can be genetically engineered to grow tumors of their own, or they can be xenograft models with patient specific tumor growth.

Genetically engineered mice are typically more expensive and time consuming because they involve altering a mouse germ line to promote oncogenes or to deactivate tumor-suppressor genes. However, they are useful when studying gene function and tumor progression pathways. In order to get a more personalized cancer treatment and develop anticancer drugs, xenografts are more useful. Xenografts are cheaper and less time consuming than genetically engineering mice, but they lack the true microenvironments that the tumor would experience in the body because they are not from the DNA. Due to this, the tumor architecture and behavior in a xenograft are not representative of the cancer in the human body [21]. While rodent models are beneficial in some aspects of cancer research, there are too many physiological differences, like the different immune systems, that prevent mice from being an entirely accurate human tumor model. On a more ethical viewpoint, there is a distinct movement away from animal testing, so there is a need for an *in vitro* model that further exceeds the benefits of using an animal model.

2.3.2. Hydrogels

To overcome limitations associated with 2D and animal models, 3D tumor models have been utilized with one of the first being created through hydrogels. Hydrogels are comprised of natural or synthetic hydrophilic polymers that absorb water when exposed to a stimulus (i.e. heat, pH, electricity, etc.) [22]. These hydrogels are highly tunable and are used to represent the native tissue's ECM that the tumor invades. The idea is that a hydrogel ECM can be created to mimic the mechanical and microenvironment of the natural tissue, so that the tumor cells act more like they would in the human body [23]. When tumor cells interact with the 3D environment, they can perform more natural cellular interactions, especially when compared to 2D models.

The mechanical characteristics are not the only factor in cell migration and tumor growth, so it is important that the hydrogel scaffold is made of the best polymer and biochemical factors that represent the naturally invaded tissue [22]. Once the cancer cells have invaded the hydrogel

ECM and created a tumor, researchers are able to test the viability of various drugs on the cancer cells without having to test them on the patient [23]. A drawback of using hydrogel scaffolds is that even scaffolding techniques do not allow for complete physiological conditions. The cancer cells interact and react with different substrates and biochemicals that they would not see in physiological conditions (i.e. collagen I). The use of hydrogels is also somewhat antiquated in the field of cancer research, but it has helped guide researchers to the use of spheroids.

2.3.3. Spheroids

The spheroid method of cell culture is ideal for rapidly proliferating cell types, especially those that are cancerous in nature. This particular method of cell culture creates a cell aggregate in a scaffold-free environment by allowing cells to grow on top of each other [24]. The morphology of a 3D cell spheroid is dependent on the cells being used in culture, however; regardless of cell spheroid size and cell line, most spheroids grow and develop in the same manner within the first 1-5 days. These cell aggregates can be generated in suspension by the forced floating method, the hanging drop method or the bioreactor agitation approaches [25]. 3D spheroid culture improves upon previous 2D and 3D culture methods mentioned because of the improved cell to cell and cell to extracellular matrix (ECM) interactions. These interactions allow cells to have more similar phenotypes to what they would *in* vivo.

In addition to this, spheroids are comprised of cells at different stages of the cell cycle and life; meaning that there are proliferating, quiescent, apoptotic, hypoxic and necrotic cells all within the spheroid aggregate [26]. One can expect to see cells at varying age and functionality because of the non-homogenous nature of nutrient exchange throughout a spheroid. In the core, cell death is due to lack of nutrient and oxygen penetration into the center. In general, a larger spheroid, of more than 500 thousand cells, experiences necrosis while, a smaller spheroid, of cell less than 500 thousand cells, do not have this issue as often. When modeling different tumors at different sizes, it is important to consider how large the cultured spheroid should be. If a goal of culture is to screen a drug, the cultured spheroid must emulate the *in vivo* size. If a drug has low penetration but excellent effectiveness, it is much more effective in a smaller spheroid than a larger one.

On the other hand, 3D spheroid cell culture is much more expensive than the traditional 2D system which makes it less accessible to startup projects. In addition to this, spheroid cell experiments may have large variability between different cultures, this makes it very difficult to have reproducible experiments and results. This is mostly because when growing up cells from well to well, the cell aggregates may be slightly different which can cause large differences in the overall spheroid. Spheroids also lack vasculature that may be present in a tumor, this means that some large tumors will never experience necrosis *in vivo* and will have much better drug permeability than a solid mass of a large spheroid. 3D spheroids are far from a perfect method of disease modeling; however, they help bridge the gap between *in vivo* disease and *in vitro* screening and testing.

2.3.3a. Hanging Drop Method

The hanging drop method allows cells to aggregate in suspension due to gravity [27]. It uses an inverted well plate promote cell growth that would be restricted by a traditional flat well and allows the cells to be examined without the possibility of being squished against the flat well [28]. This approach is relatively simple and inexpensive, depending on the type of equipment used. The spheroids produced through this technique are easily accessible and are nearly 100%

reproducible [24]. The user is also able to control the number of cells within the spheroid, ultimately controlling the size of the spheroid [29]. This approach, however, is met with several problems. It can be somewhat labor intensive, and it can be difficult to exchange the cell suspension medium without disturbing the cells, possibly leading to a low output of cells [24].

2.3.3b. Cell Agitation Method

The cell agitation method uses either a spinner flask bioreactor or a rotational culture system for cell suspension [24]. These containers are constantly in motion by gentle stirring or by rotating the container. This motion prevents the cells from adhering to the walls of the container and promotes cell to cell interaction to form spheroids. The cell agitation approach is a simpler method for culturing cells and can easily be scaled up for large-scale production. The spheroids produced from these methods are easily accessible and the constant motion of the fluid can help with nutrient transport. This approach, however, can be very expensive and the user has no control over the size of the spheroid or the number of cells within the spheroid [29]. With these advantages and drawbacks, this approach closely resembles the human body due to the shear forces present and constant motion that cells would typically experience inside the body.

2.3.3c. Forced Floating Method of Cell Aggregation

The forced floating method to create 3D cell aggregates a simple, dependable and reproduceable method of spheroid assembly. This method of cell aggregation is made possible by ultra-low attachment surface modifications which prevent cells from adhering and growing on the bottom and edges of a well plate [25]. When the cells are unable to attach to the wells, cells form cell-cell interactions which allow them to aggregate. In most cases, the surfaces of the wells are coated in a poly-hydroxyethyl methacrylate (poly-HEMA), which is a very hydrophilic polymer and thus prevents cells from forming attachments to the surfaces. Once the cells are added to these wells, the cells are centrifuged over hours and days until they self-aggregate into spheroid cultures [30]. Once they have aggregated the can be relocated into a different well for longer term culture for growing up or screening of drugs. Long term culture of these cell aggregates can be achieved, up to 20 days, when exposed to the correct conditions.

2.3.4. 3D Ring

3D ring, or micro-ring, models can be used to aggregate cells within a CAD modeled ring shape (Fig. 2.1). They can be utilized alongside 3D spheroid cell culture methods listed above to generate cells in suspension. They especially work well with the hanging drop method because the ring model can allow the user to overcome the difficulties with exchanging the culture media [31]. The micro-ring model is also one of the best methods for stabilizing droplets against mechanical perturbations and over long periods of time [32]. This model also provides good nutrient exchange, which eliminates the chance of necrosis. Excluding media changes, this model does not require any scaffolding, so this culture method is self-sustaining.
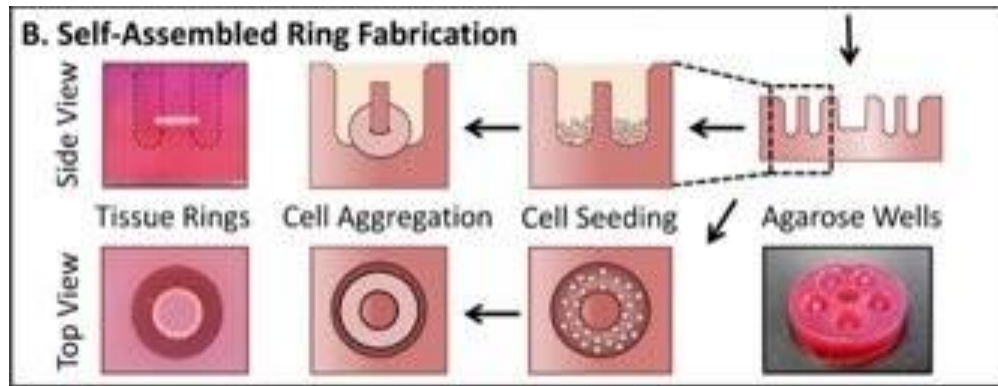
Fig. 2.1. Example Ring Model and Cell Aggregation: Figure shows a schematic of the process of using agarose ring wells to form self-assembled tissue rings [33].

2.3.5. Transwell Plates

Transwell plates are 3D models typically used to show how one type of cell or biomolecule influences another through a permeable membrane [34]. Cells in transwell plates can absorb nutrients through their basal membranes as they would *in vivo* and transport of nutrients and related metabolic activities can be clearly observed. Cells and ECM are able to pass through the well membrane. Cells pass through the membrane analogous to passing through a leaky endothelium *in vivo*. These models are easy to implement, have low cost assays, high throughput and can be used to compare metastatic function of cells.

Regarding 3D cancer cell culture, transwell models can be used to observe cancer metastasis through a membrane as well as how cancer treatments or therapies move through a membrane and influence the cancer cells on the other side. An example of this is seeing how natural killer cells will migrate through the transwell membrane and begin to break down a spheroid tumor (Fig. 2.2).

Fig. 2.2. Example Transwell Model of Tumor Cytotoxicity: Transwell plate structure and use diagram showing the migration of one cell type through a membrane towards a cell spheroid [34].

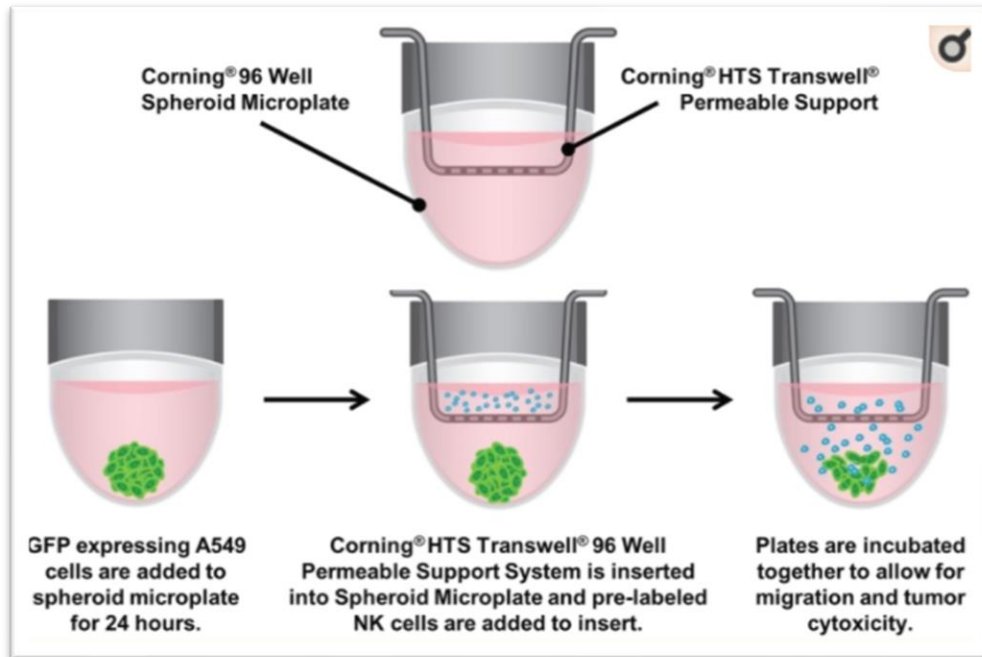Being able to observe how a treatment method will cross through membranes and be able to influence cells on the other side is useful for testing cancer treatments outside of the body. Before testing potential treatments, it is also important to determine the metastatic potential of the cancer cells being studied, which could be easily observed via a transwell model. In such a model, we can begin to see how fluid exchange affects particle and cell movement. This can be more deliberately manipulated to match living system conditions with inclusion of microfluidic aspects within the model system.

2.3.6 Microfluidics

Microfluids can range from simple to complex system that accurately mimic *in vivo* 3D microenvironments. They can control chemical gradients, fluid-based stresses, and help promote true cellular function [35]. In cancer models, certain flow conditions are important for more authentic cancer cell function, including metastasis, which will show how the extracellular factors of a cancerous system affect healthy cells and tissues. When it comes to cancer treatment models, microfluidic systems are important for anti-cancer drug screenings and seeing how the tumor and surrounding healthy tissue physiology changes. Microfluidic systems have a wide range of designs. The following example shows a basic set-up to observe how fluid flow affects cancer metastasis (Fig. 2.3).
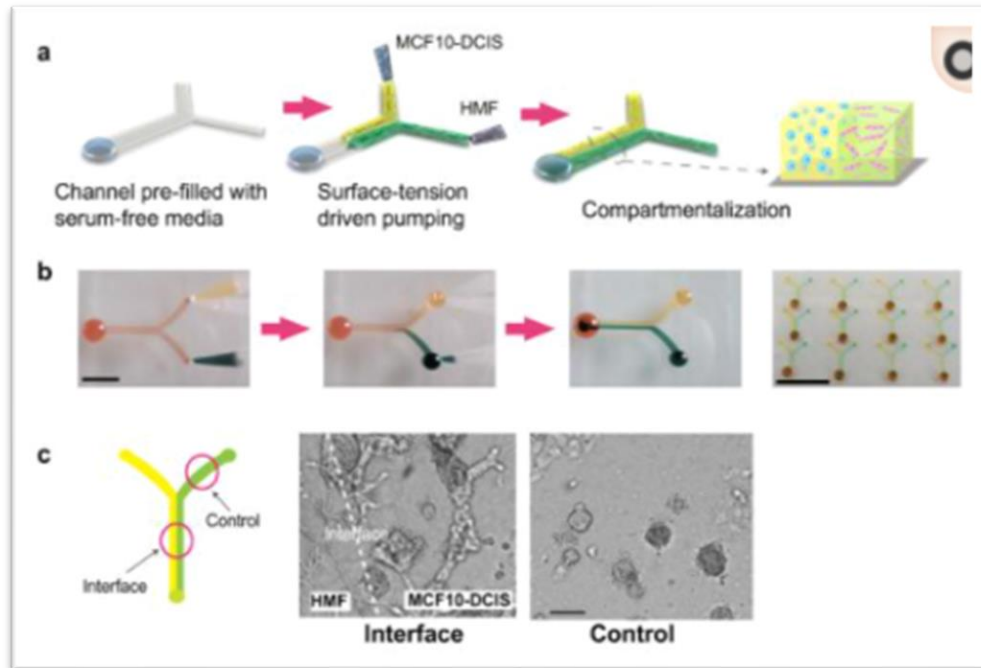
Fig. 2.3. Example Microfluidics System Modelling Breast Cancer Invasion: A microfluidics system to analyze the effects of fluid flow and surface tension on cancer cell invasion [35].

The diagramed system includes a compartmentalized tubing which utilizes breast cancer cells to show cancer metastasis. Fluid flow through the compartments is driven by passive pumping based on surface tension. One side has cancer cells and the other has healthy cells. The fluid flow through the compartmentalized system showed that the cancer was able to influence the healthy tissues even when physically separate. This process would have not been as accurate to *in vivo* conditions if there was not extracellular fluid flow as there is in the body.

2.4. Personalized Medicine

Personalized medicine has taken the medical community by storm since the early 2010s, people more and more have moved to a personalized approach of disease prevention, diagnosis and treatment [36]. In typical treatment of cancerous tumors, medical professionals generally follow a course of cancer treatments that has been standardized for each type of cancer. When a patient is diagnosed with cancer in a specific stage, there is a protocol to follow almost indiscriminately. For these treatments, only about 40-50% of cancer cases clear, the other half's cancer is either unaffected or did not respond well [2]. Following a lack of response, many medical professionals will move to a combination of treatments to try to wipe out the cancer. This method, while sometimes effective, is hard on the body and it is hard to see which treatment yielded the desired positive response from the cancer.

To remedy this issue, there has been a push to apply more personalized medicine techniques to cancer treatment. Personalized medicine is based in the idea that every person is different and in order to properly treat that person, the medical professional should look at every case as novel. Medicine can be personalized through genetic testing, biomarker testing and personalized disease modeling [37]. Genetic and biomarker testing can assist in preventative medicine through risk assessment, early detection, and diagnosis of many diseases. Once a

person is diagnosed with a disease, personalized medicine can help with medication selection, choosing the safest dosage and improving drug development, all based on a person's specific genetic profile. Personalized disease modeling is slightly different, this method is mostly used for treatment purposes, to treat the person with the most effective drug or method on the market the first time around. This is achieved by modeling a person's disease characteristics and trying different treatments for it *in vitro* so they can ensure they have the right medication to be used *in vivo.* Overall, personalized medicine holds much promise for improving efficacy of cancer treatment options on a person-to-person basis.

3.0 Project Strategy

This section outlines the intended milestones of our research. This includes our initial and revised client statement and project objectives intended to work towards our overall goal. This section also briefly describes project design requirements, constraints, and an estimated timeline of our research.

3.1 Initial Client Statement

Most cancer types have a variety of treatment options, including chemotherapy, radiation therapy, hormone therapy, and targeted immune therapy. Although this range of treatments exists, each individual patient's cancer responds differently to various treatments. Ineffective treatment attempts can be detrimental to healthy tissues and the overall health of the patient. There is a need for a more accurate method to allow doctors to test and develop more effective treatment options against primary and metastatic cancer. A personalized 3D tumor model, complete with accurate cancer cell function and metastasis, will allow for treatment testing of an individual's cancer prior to application to determine the most effective cancer therapy beforehand.

3.2 Objectives & Constraints

In order to address the need for improved cancer treatment in a variety of patients, we aim to create a multi-cell type, contiguous tissue 3D tumor model. Our first objective is to perform 2D cell culture of healthy cells and cancerous cells. This will allow us to observe potential differences in proliferation and cell function between each type of cell culture.

After this initial assessment, we will utilize and manipulate cell self-aggregation properties to form 3D shapes. The cancerous cells will be formed into spheroids to mimic a tumor cell cluster. The healthy connective tissue cells will be formed into rings. The cells will be shaped to form tissues that will represent a tumor microenvironment, including surrounding healthy cells.

A combination of the above shapes will be formed and monitored for cancer cell integration into the 3D tissue. Microscopy will be utilized to observe integration, migration, and invasion of cancer cells. It is important that our model shows definite and accurate metastatic function comparable to metastatic patterns as observed *in vivo*. Metastatic behavior of the 3D model must be replicable to a certain degree of precision and accuracy to naturally occurring metastasis.

Our final objective is to assess whether our chosen 3D model type and methods work best to mimic *in vivo* tumor environment. We will also review our techniques and outcomes to assert whether our model could be used in patient specific modelling and treatment testing. This determination will require multiple series of 3D model creation and testing to ensure tumor microenvironment accuracy and faithful reproducibility.

A major factor in the completion of this project is laboratory availability. Due to the COVID-19 Pandemic, laboratory time is limited which effects our cell culture strategies and could negatively impact our ability to perform repeated trials of modelling and metastatic assays. Secondly, the laboratory available to us has a limited supply of various materials for our use. Our project budget is $1000 which also limits what materials, and amounts of materials, we can use over the duration of our research. To limit costs of custom materials, our design should be compatible with standard materials and equipment that can be found in a typical biosafety level 2

laboratory space. On the technical side, all aspects of our project design need to be kept sterile as we work with cell and tissue cultures.

3.3 Design Requirements

This section outlines requirements that must be met and withheld over the course of the project, including ISO guidelines, FDA guidelines, and good cell culture practice.

3.3.1 International Organization for Standardization (ISO)

The International Organization for Standards is an international organization that oversees the industry standards for innovations in the making, managing, and delivering of a product or service. These standards are agreed upon by experts from 164 different countries that discuss and inform others on best practices in varying fields [38]. Even without a definitive project design and methodology, some general standards that must be considered over the development phase of this project are ISO 13845:2016, ISO 11737-2:2009, and ISO 20916: 2019.

ISO 13845: 2016 is a regulatory standard for all medical devices. This standard ensures that each step in a medical device's design and manufacturing process is done with quality. It oversees that medical device involved organizations are consistently meeting the regulatory and customer based requirements [39]. For our project, any structure that is manufactured to aid in the creation of the tumor model is considered a medical device, and therefore must follow the regulations presented in ISO 13485: 2016. Along with the structure, the tumor model itself is considered a medical device, so it would also be upheld by ISO.

ISO 20916: 2019 is specifically for *in vitro* diagnostic medical devices, like our tumor model. More specifically, this standard lays out regulations for working with specimens from human subjects during clinical studies. These regulations are to be followed to "protect the rights, safety, dignity and well-being of the subjects" during clinical studies [40]. This standard can also be used to help design the study to ensure subject safety and data integrity. Each subject sample needs to be handled in a manner that allows for reliable and significant results for the study.

In the formation of various structures to include or use in making our 3D tumor model, we will have to abide by ISO 11737-2:2009. This standard identifies sterility testing criteria on medical devices. It is to be used when designing and validating a sterilization process [41]. We will utilize this sterilization standard for any material that we use in our tumor model culture.

3.3.2 Food and Drug Administration (FDA)

For our design to reach the market, it must first be validated and approved by the Food and Drug Administration (FDA). The FDA "is responsible for protecting the public health by ensuring the safety, efficacy, and security of human and veterinary drugs, biological products, and medical devices" [42]. Since our project will be a medical device, it is included in the scope of the FDA. All medical devices are further classified into class I, II, or III. Each class has its own subset of regulations and exemptions, but all must be FDA approved before they can be used by consumers.

3.3.3 Good Cell Culture Practice (GCCP)

To have successful proliferation and growth of cells and tissues we will utilize in the formation of our tumor model, we must employ Good Cell Culture Practice (GCCP). The

principles of GCCP include "establish and maintain adequate measures to protect individuals and the environment from any potential hazards … assurance of the quality of all materials and methods, and of their use and application, in order to maintain the integrity, validity, and reproducibility of any work conducted … document the information necessary to track the materials and methods used, to permit the repetition of the work, and to enable the target audience to understand and evaluate the work … compliance with relevant laws and regulations, and with ethical principles … provision of relevant and adequate education and training for all personnel, to promote high quality work and safety" [43]. These principles will allow us to perform culturing of engineered tumor tissue in a safe, replicable, and validated manner.

3.4 Revised Client Statement

The gap in cancer treatment success rates can be addressed by an accurate, *ex vivo*, 3D tumor model. Development of a patient-specific 3D tumor model can be used in treatment testing to see the effects on an individual patient's cancerous and healthy cells. This can reduce the trial periods of cancer therapy being administered directly to the patient and can reduce the harmful effects of various cancer treatments. The result of being able to test numerous therapies on a model system is the ability to determine the optimal treatment type to administer to the patient with limited negative health effects.

3.5 Project Approach

Due to the limited time in which our group must complete our objectives, we created a detailed Gantt chart to provide a project timeline and ensure the project progresses at the appropriate pace (Fig. 3.1). Additional weekly times were set aside for group meetings and meetings with our project advisor to ensure the group is maintaining progress, staying organized, and keeping open communication. All laboratory applications are held in Goddard Hall 006 at Worcester Polytechnic Institute.

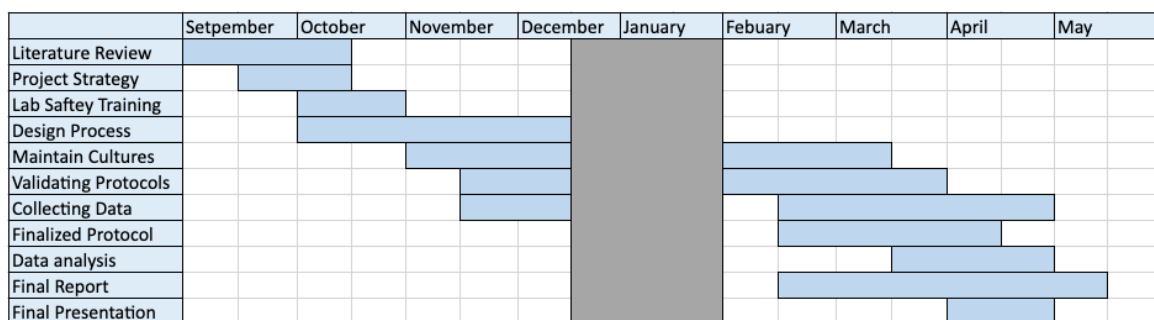|	Setpember	October	November	December	January	Febuary	March	April	May
Literature Review									
Project Strategy									
Lab Saftey Training									
Design Process									
Maintain Cultures									
Validating Protocols									
Collecting Data									
Finalized Protocol									
Data analysis									
Final Report									
Final Presentation									

Fig. 3.1: Gantt Chart: This chart shows the proposed timeline for our project over the course of the year.

4.0 Design Process

The focus of this section was to present the team's reasoning behind the project design and the process of making this decision. Several studies were reviewed to help the team narrow their decision and a general treatment plan was constructed. This section will further discuss the conceptual designs for this treatment plan, potential prototyping models, and feasibility studies for the final design.

4.1 Needs Analysis

To create an accurate *ex vivo* 3D tumor model and to ultimately help develop methods of personalized cancer therapy, the group created a set of requirements needed for our design. These requirements were established by studying previous research done on disease models and determining how we could improve them. Current disease models inaccurately mimic the human microenvironment and how it would respond to current treatments. We hope that our design requirements allow us to develop a model that more accurately mimics the human microenvironment, is easily replicable, has minimal cell necrosis, is adaptable to various experimental testing and cell types, and only requires culturing for a short time period. These requirements were weighted and evaluated using a Pugh Model. The Pugh Model is a popular evaluation and selection method that allows the user to assign a quantifiable measure to their design criteria. Our design requirements and weight values are listed in Table 4.1.

Table 4.1 Design Requirements for 3D Tumor Model: The importance of various design requirements was listed and ranked based on importance from low (1) to high (5).

Requirements	Weight
Easily repeatable	5
Low time in culture	3
Accuracy to *in vivo* 3D state and microenvironment	5
Ability to be used for different cell lines – personalized to the patient	4
Cost of culture accessible for multiple trials	2
Minimal necrosis	3

Each of the requirements were weighed in a scale from 1 to 5 to determine their importance in respect to our final design. A rating of 1 indicated low significance and a rating of 5 indicated very high significance. The requirements to generate a tumor model were ranked in order of most important to least important, some of these included the ease of replicability, accuracy to the *in vivo* state and microenvironments were ranked as the most important requirements to meet. The ability to be used for different cell lines and personalized to each individual patient is important for the scope of our design and was ranked a 4. A model that produces minimal necrosis and requires a low time in culture is somewhat important and were both ranked at a 3. Finally, developing a model at a feasible cost in order to run multiple trials is not as important as the other requirements, but enough to be considered, so it was ranked as a 2. Our team believes that by following this needs analysis, we would be able to design a strong 3D tumor model to help further develop methods for personalized medicine.

4.2 Design Concepts

With the overall need being a way to improve treatment outcome in cancer patients, our team investigated the different areas for possible design (Fig. 4.1). We determined that the three principal areas to address this need are treatments, improve diagnostics, and disease modeling. While there are many treatments and methods of diagnosing patients, we believe the area that is the most underdeveloped is disease modeling. From here, we separated disease modeling into *in vivo* and *in vitro* studies. Since another goal of our project was to make the model personalized to the patient, the more viable option was *in vitro* modeling. Based on our background research, we determined that a 3D scaffold-less design would be the best option.
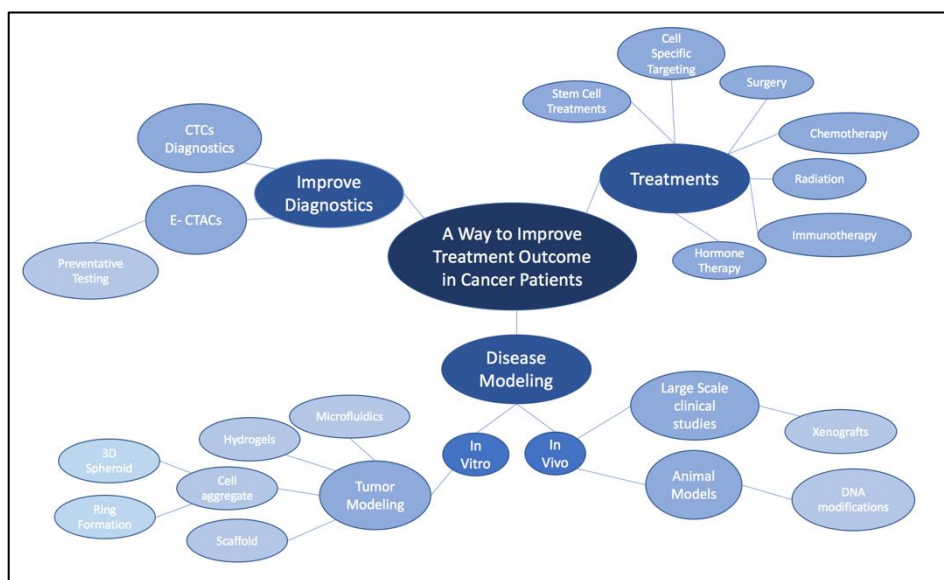

Fig. 4.1: Concept Map: A visualization of various aspects that can contribute to improving cancer treatment outcomes.

4.3 Alternative Designs

The following section discusses initial designs that could be used to create an accurate 3D tumor model. These designs are later evaluated based on our needs criteria for the project.

4.3.1 Scaffold Model –Hydrogel

This design utilizes a hydrogel that could then be seeded with human primary breast tissue fibroblasts derived from a healthy 52-year old female (HMF-52) and MDA-MB 231 GFP cells. This would provide a 3D base for the cells to attach, grow and proliferate within. A study by Li et al. used hydrogel scaffolds to form a medium for breast cancer spheroid growth for use in disease modeling models [44]. Fig. 4.2 below shows the progress and structure of a hydrogel scaffold containing cancerous cells that will form cancer cell spheroids. The downsides to this are cost of forming the scaffold and reliable nutrient exchange throughout the system. Cells may not seed correctly and could negatively impact cell growth and behavior and because using a matrix is less feasible, replicability of this design would be low.
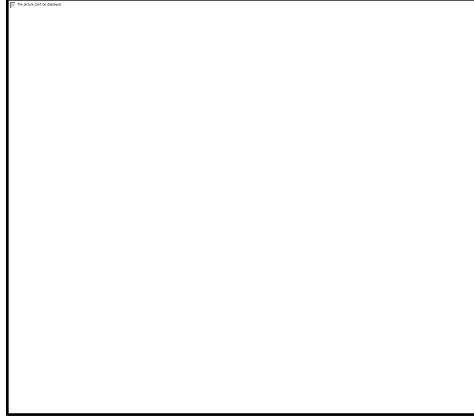
Fig. 4.2. Hydrogel Tissue Scaffold for Cancer Modeling: An example of cancerous cell culture within a hydrogel that will create self-aggregated spheroids [44].

4.3.2 Spheroid Model

The spheroid model design entails a cluster of cells that have aggregated into a mass of cells. Specifically, this 3D culture method would be used in a co-culture system with HMF-52 fibroblast cells and MDA-MB 231 GFP breast cancer cells. This spheroid could be recapitulated in any number of ways: it could be a simple co-cultured spheroid, or a fibroblast spheroid and then have the cancerous cells added to monitor migration and invasion of cells into, or out from, the spheroid (Fig. 4.3). One of the fundamental issues with the spheroid tumor model is lack of vascularization and nutrient exchange into the spheroid. This can lead to necrosis in the center of the spheroid, this is not necessarily like the *in vivo* state and will effectively end the culture. Additionally, the spheroid model will have penetration issues when preforming drug screening, making it not the most ideal 3D culture system for future cancer therapy evaluations.
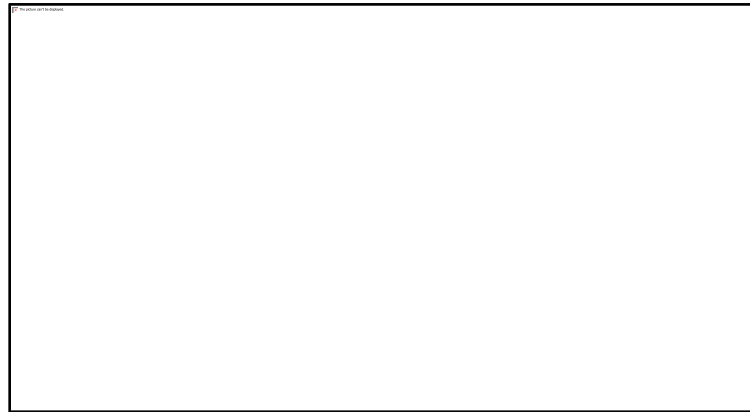

Fig. 4.3. Cell Spheroid Model: An example of cell culture utilizing a co-culture of two different cell types [26].

4.3.4 Various Shape Cell Aggregates

We believed there could be some merit to testing how various shapes to form cell aggregates could affect the resultant tissue. For preliminary testing of shapes, we formed a test 24 well-plate including rings, triangles, and hashtag shapes (Fig. 4.4 and Fig. 4.5). Each shape, once used to form an agarose mold, would include a central post with a 2.5° inward taper. The

27

difference in shapes would mainly show us where cells prefer to aggregate – at points of high vs low stress – and which shape produces the most uniform tissue. This design would also warrant testing how many cells are required to form aggregates dependent on each shape. There is a range of one to four posts set for each shape in different wells. A different number per well could show us how many posts per well is most efficient, in both making the agarose mold with high resolution and in seeding cells.
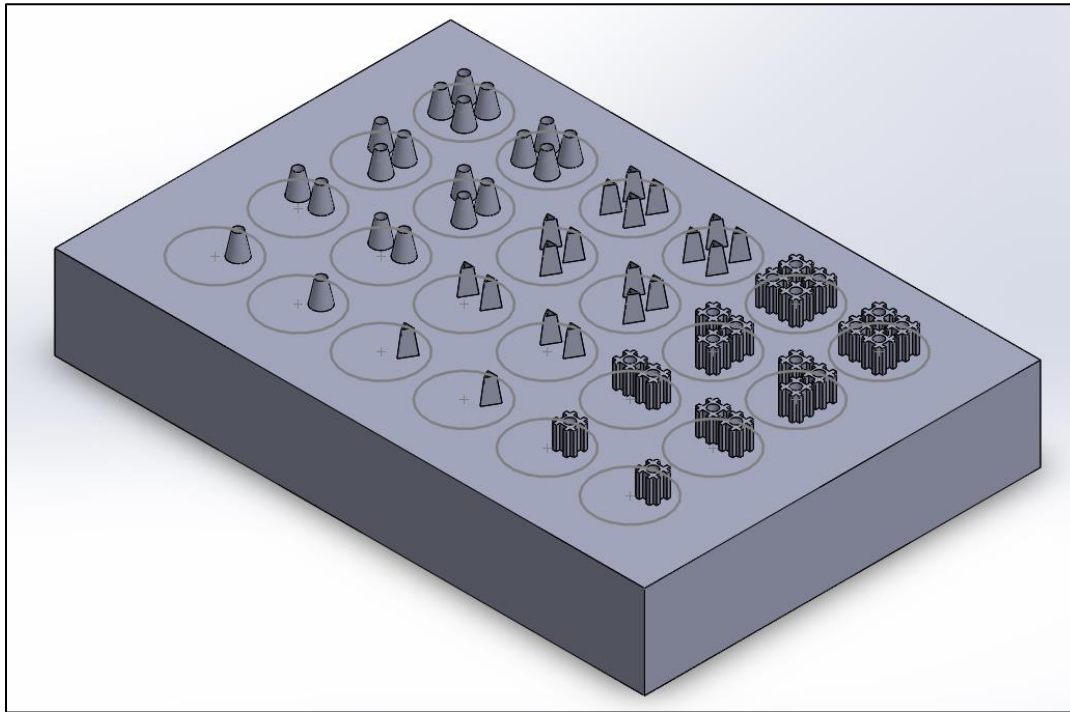

Fig. 4.4. Multi-Shape Cell Aggregate Plate: This piece would allow for cell aggregate formations in various shapes, circular ring, triangle, or hashtag, over the entirety of a standard 24-well plate.
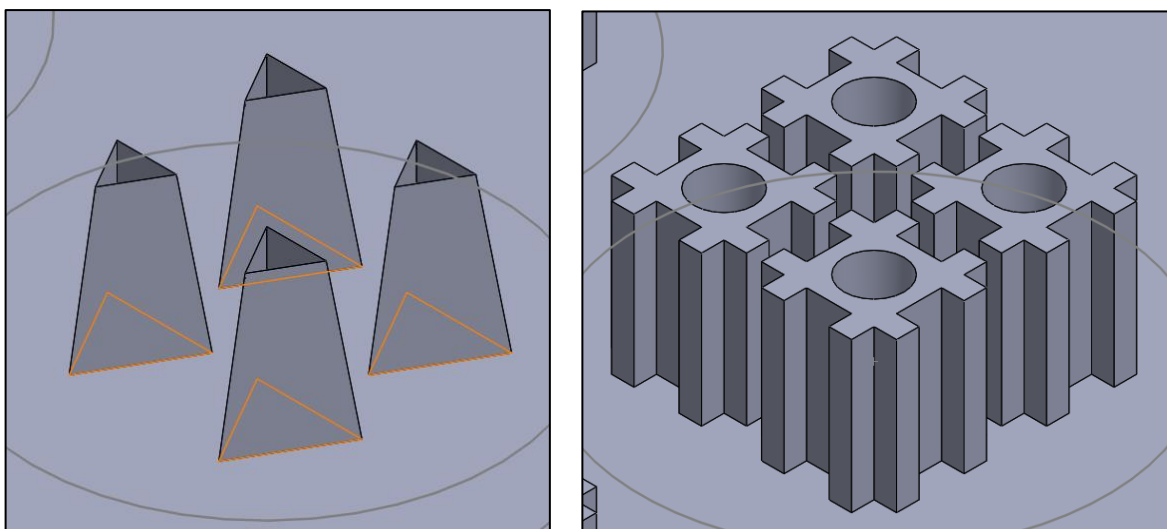

Fig. 4.5. Zoomed Images of Triangle (left) and Hashtag (right) Posts: Focused images of the triangle and hashtag punch shapes for formation of more unique cell aggregate forms.

4.3.3 Tissue Ring Model

The tissue ring model involves the creation of an agarose mold in which the tissue ring will form around a central agarose post with a 2.5º inward taper (Fig. 4.6). The ring structure is ideal for mimicking the *in vivo* state because of the cell-to-cell interactions within the ring. Additionally, this ring has limited risk of necrosis even with large cell numbers composing the ring. One of the concerns about the ring structure is the replicability. Through speaking with Professor Rolle of WPI, we were informed the ring structures are specific in the volume of cells used to produce them. Meaning if there are not enough cells, the rings will not form and if there are too many they may burst. Part of developing this design will include finding the correct balance of number of cells and the best ratio of fibroblasts to cancer cells for uniform ring formation.
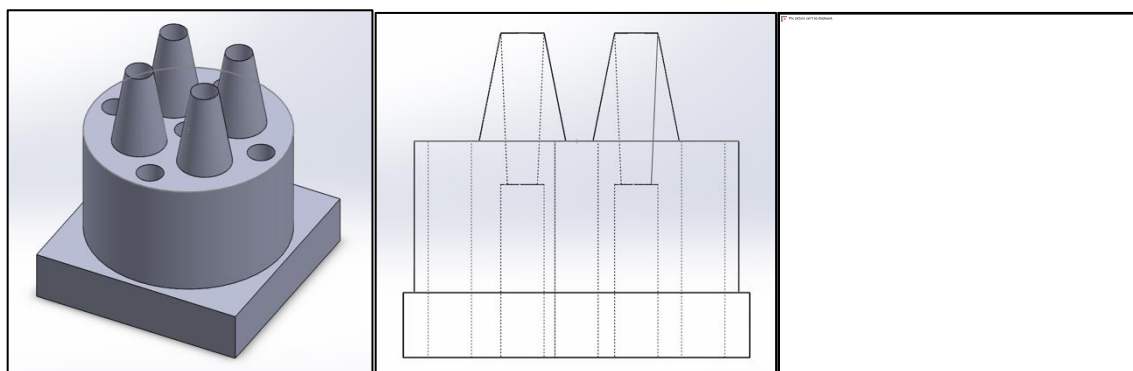

Fig. 4.6. SolidWorks Model of Component to Form Tissue Rings: These are the rendered images of our final tissue ring punch design. From left to right are the isometric view, front view, and top view to show the cones for ring formation and the through holes for air displacement.

4.4 Final Design Information

After considering potential designs, we selected the strategy that best suited our needs. Our selection process and rationale are detailed below, along with a full explanation of our methods for tumor model formation.

4.4.1 Previous Research

Previous studies into cell clusters and self-aggregation have been completed to explore different tissue models with muscle cells. Initial studies were completed in Professor Rolle's lab where they explored the use of human smooth muscle cells seeded into rings to mimic human blood vessels. The investigators chose this method to more accurately promote the 3D and scaffold free environment that blood vessels would typically be found in. With a blood vessel made of fused rings, they were able to more accurately represent vascular diseases that only affect localized points or areas of cells along the blood vessels [45]. Following their success to create blood vessels, the investigators expressed the need for this technology to be used in high throughput screening, and to be used to study the various localized vascular diseases.

Using a similar tissue ring method, Jason Forte of Professor Page's Lab at WPI investigated creating skeletal muscle micro tissues that mimicked those in the human body. Previous 3D models of human muscle tissue lacked similarity to the natural environment due to core necrosis and inaccurate extracellular matrix components. Forte was able to successfully

create human muscle cell tissue rings that accurately represent human muscle tissue in respect to cellular behavior and mechanical properties. With this success, these rings can move on to be trialed in studies of skeletal muscle diseases to more accurately predict the efficacy of drugs in candidate specific microtissues [45].

In both studies, a 2% w/v agarose mold was used to grow the tissue rings. Forte discovered that the rings were bursting after a short period of time in culture using the protocol from Professor Rolle's lab. In order to combat this, Forte supplemented the media with adult horse serum to reduce proliferation and force the cells to make their own extracellular matrix. He also determined that wells made with a 2mm post tapered at a 2.5° angle created the best tissue ring formation results [46]. This degree of taper of the center post allowed for the aggregating ring structures to move upward on the posts as the cells contract together. This upward movement allows some tension to be relieved from the rings and prevent ring rupture.

The successes in these two studies laid the groundwork for our project. Using protocols and measurements from the two studies, we can better understand how to make a tissue ring that is phenotypically similar to the tissue *in vivo*. The goal of each of the projects mentioned is the same: to create a diseased tissue model that can be used for researching various treatments and diagnostics of the disease.

4.4.2 Final Design Selection

After going through several design alternatives, we limited our final design selection to four main design options. These included the decellularized tissue scaffold model, the spheroid model, the ring model and the alternative shape model (we focused on the triangle). We compared each of the designs and scored them based on what we determined from our needs analysis (Table 4.2). The most suitable model for our needs was found to be the ring model. The ring model is most similar to the *in vivo* state because of cell-to-cell contact, without creating an environment susceptible to necrosis. The ring model is not without its issues, specifically, when looking into replicability between ring structures. Even in consideration of this, the ring structure was the model that best matched our needs.

We found that the spheroid model and the scaffold model were the least applicable for our needs. The scaffold model does not have good accuracy to the *in vivo* state because of the lack of cell-cell interactions due to proliferation on the scaffold. The spheroid model also did not meet our needs in terms of necrosis. The literature has indicated that spheroids over 500 thousand cells are very susceptible to necrosis [24]. The triangle model scored 22 making it the second-best option based on our needs. The triangle is like the ring model in satisfying many of our needs, however, the triangle structure is more likely to fail around the sharp corners of the triangle mold, making it hard to replicate. Additionally, the stresses around the corners of the triangle are not necessarily like the *in vivo* state.

Table 4.2. Final Design Decision Matrix and Key: Using a color-coded ranking system, the design that best suited previously determined requirements was chosen as the final design concept.

	Scaffold Model	Spheroid Model	Triangle Model	Ring Model
Easily Repeatable	4	4	2	3
Low Time in Culture	4	4	4	4
Accuracy to *in vivo* state	1	3	2	4
Personalized to patient	4	4	5	5
Cost of culture	3	4	4	4
Minimal Necrosis	4	1	5	5
Total	20	20	22	25

Key	1: Bad	2: Poor	3: Average	4: Good	5: Excellent

4.5 Final Design

Based on the decision matrix in the previous section, we proceeded with our Tissue Ring Model. Figure 4.7 shows our 3D printed, single well punch that we used to form our agarose rings and posts. The 3D printed part was formed of durable resin with glossy finish and printed using the Objet 260 Connex machine at WPI. There are air holes in the main block and through each of the posts to allow for proper placement and mold formation in the agarose. The 3D printed piece can be sterilized with 70% isopropanol.
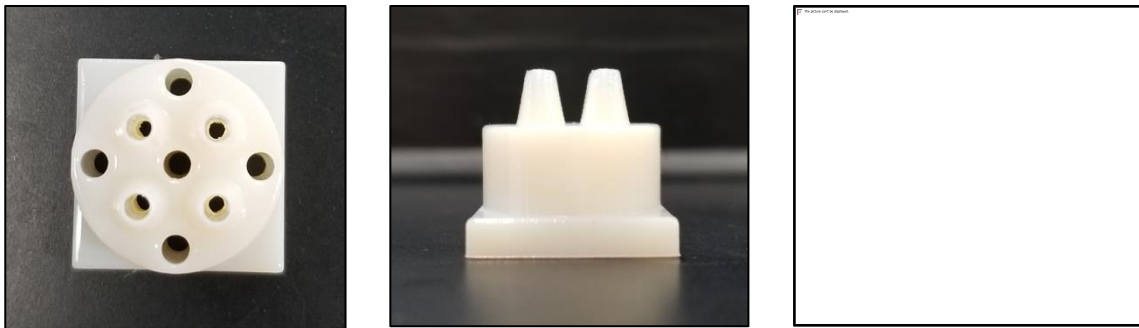

Fig. 4.7. 3D Printed Component for Tissue Ring Model: Various views of the 3D printed punch used in agarose gel ring well formation.

The agarose shapes for seeding will be formed one well at a time in a 24 well-plate, leaving 4 rings in each well. The punch will create a 2mm diameter central post, tapered inward at a 2.5° angle. Holes leading all the way through the punch are necessary for pressure release and allow for agarose to move into the cones and make posts. The square base rests at the top of the well for stability and to prevent the punch from sinking as the agarose cools. Once the agarose set, the punch was removed. The result are four ring wells with center posts capable of holding solution to encourage cell self-aggregation into tissue rings (Fig. 4.8). The agarose was

previously sterilized via autoclave so this formation and subsequent seeding of cells will take place in the biosafety cabinet.
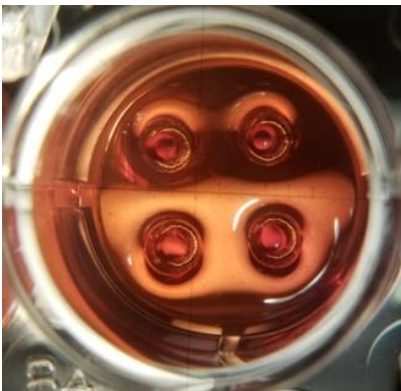

Fig. 4.8. Agarose Gel Ring Wells: This image depicts the four agarose gel ring wells that result after use of the printed punch. This image is taken at 0.8x magnification.

4.6 Final Design Methodology

In order to obtain our final goal of a cancerous and non-cancerous co-cultured tissue ring, we needed to perform experiments that would help accomplish our objectives. For the co-cultured tissue ring, we wanted to perform a co-culture of HMF-52 fibroblasts and MDA-MB-231 tumor cells in both a suspension culture and a co-culture with a fibroblast ring and an MDA-MB-231 spheroid cultured into the ring. The MDA-MB-231 cells were already transfected with GFP, so we knew we could utilize the fluorescence microscope to identify the unique behaviors of both cell types. In order to address our first objective, we routinely sub cultured and passaged out HMF-52 and MDA-MB-231 cell lines according to the protocol outlined in Appendix A. Because we knew we wanted to utilize an MDA-MB-231 spheroid, we completed hanging drop protocols outlined in Appendix B. We seeded varying cell densities in drops on the lid of a cell culture plate, and carefully replaced the lid. We used microscopy to image these hanging drops over the course of set time frames. These various hanging drop experiments helped us to better understand how long we would need to allow the cells to self-aggregate, as well as which seeding density would be appropriate to fit within our ring molds.

The final ring punch mold needed to be tested for its ability to create replicable ring molds in agarose. Chapter 4.5 describes how the punch was used, and throughout our trials, we modified the CAD design and 3D printed model to create wells that were easily created and were consistent in shape. The full agarose ring protocol can be found in Appendix C. Successful ring well creation helps to partly accomplish objective 2 by making molds for cells to aggregate into 3D structures.

Before we performed a co-culture, we needed to determine how long it would take for the tissue rings to form, and how many cells we would need to seed in order to create sufficient and strong tissue rings. We seeded multiple cell densities into the agarose ring molds and monitored their growth and behavior over the course of a set time frame. This experimentation helped to complete our second objective and a full protocol of the tissue ring formation can be found in Appendix D.

The final experimentation performed with our ring molds was the co-cultures of the MDA-MB-231 cells and the HMF-52 cells. For the suspension trials we created a cell mixture of

both cell lines and seeded them into the ring molds (Appendix E). For the spheroid co-culture we seeded HMF-52 cells into the molds and transferred an MDA-MB-231 cell spheroid from a hanging drop into the same ring mold (Appendix F). Both co-cultures were imaged over a set time frame, and fluorescence microscopy was used to better understand how the MDA-MB-231 cells and HMF-52 cells interacted. Analysis of this experimentation can be used to complete our third and fourth objectives. A schematic of our co-culture experimentation can be found in Fig. 4.9.

Fig. 4.9. Schematic of Co-culture Tissue Ring Formation: This figure shows each of the steps involved in creating the MDA-MB-231 and HMF-52 cell tissue ring.

Over the course of determining our final design and protocol, we conducted a variety of tests to verify assumptions about our project. These experiments were also to determine the validity of various elements of our project plan in working towards our overall goal.

5.0 Design Verification and Validation

        This chapter outlines the results of various points of experimentation over the course of our research. To better understand how the fibroblast cells and the cancer cells interact with themselves and each other, we conducted cell aggregation experiments, co-culture observation, and migration assays. These results are significant to determine what is effective in creating an accurate 3D tumor model, as well as what further research can be conducted in the future.
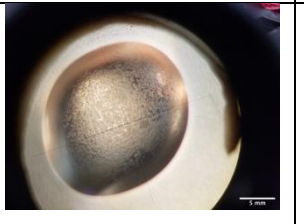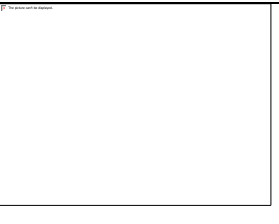
5.1 Hanging Drop Spheroid Formation

        The hanging drop method was used to determine whether the two cell lines would self-aggregate (see Appendix B for procedure). Various trials were conducted to affirm self-aggregation and to test optimal spheroid cell densities for our purposes.

5.1.1 Spheroid Cell Density Tests

        We formed MDA-MB-231 cell spheroids at various cell concentrations (Table 5.1). This experimentation was to help us determine what cell densities were most uniform and had the best self-aggregation. The most promising spheroid concentrations were chosen for future trials.

Table 5.1. Spheroid Cell Density Limit Test: This shows the comparative morphology of MDA-MB-231 cell spheroids at densities ranging from 25K to 240K cells per 20µL. Images are taken at 3.2x magnification.
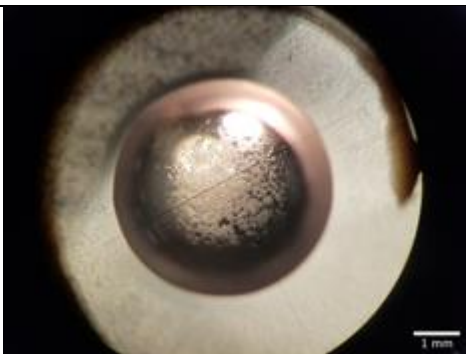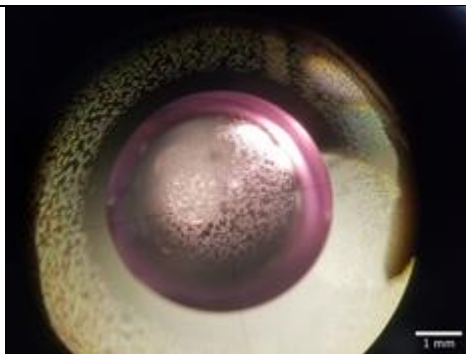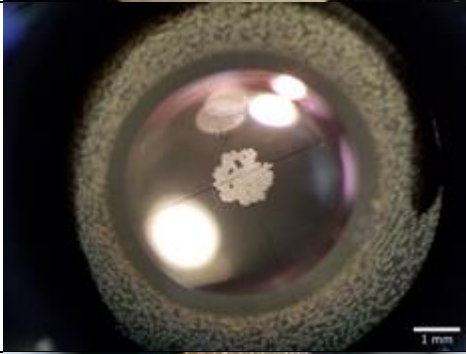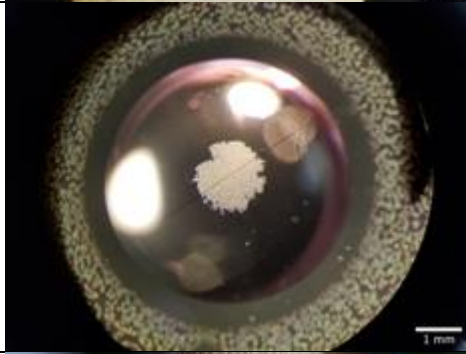
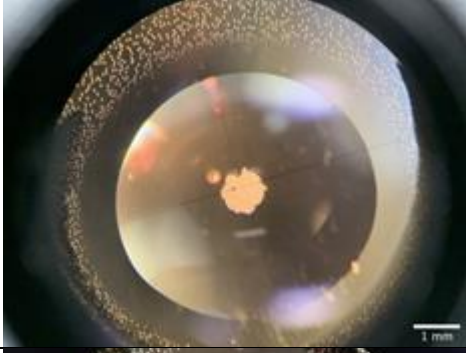| MDA-MB-231 Cell Number per Spheroid			
25K	50K	120K	240K
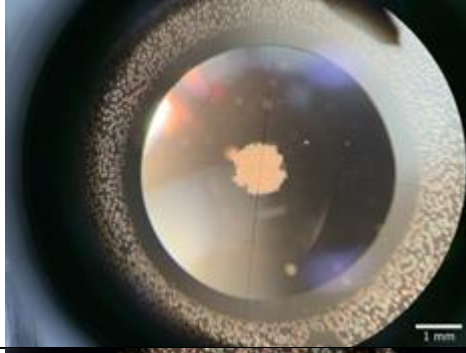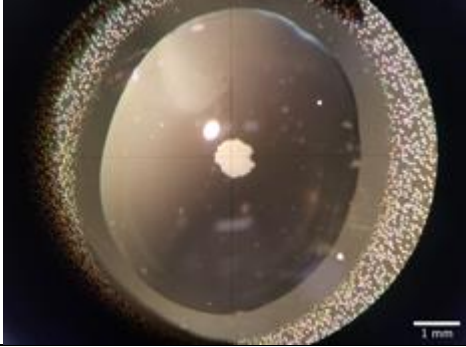
        Each droplet of cell suspension used in every trial was 20µL. Based on our observations, the 50K cell spheroids were most uniform, which includes an even, round edge, and even cell density across the sphere. The spheroids with fewer cells were not as uniform, had cell clusters that were not part of the main spheroid and had holes. The porous appearance of the 25K cell spheroids were not as uniform as the 50K cell spheroids, however, the porous spheroids may be beneficial for use in a 3D model because they allow for greater nutrient exchange with the surrounding cell environment. The 120K cell spheroids were far too concentrated. The cells did not make a uniform, condensed spheroid. From our trials, 120K was the upper limit of cells per drop.

5.1.2 Extended Spheroid Culture

        Over the course of 7 days, we imaged and monitored the progression of MDA-MB-231 spheroid formations (Table 5.2). The purpose of this was to observe self-aggregation phenomena as the spheroids remained in their hanging drops. By monitoring spheroid formation over time, we were able to decide which cell density, and at which stage the spheroids would be most viable for use in integration into a tissue ring.

Three relatively uniform spheroid were selected from each batch of hanging drops to monitor and image. Below (Table 5.2) are selected images of one spheroid per cell density group that were imaged for seven consecutive days. Images shown are for days one, three, five, and seven.

Table 5.2. Seven Day Spheroid Study: Comparative images of MDA-MB-231 cell spheroids in hanging drops at two densities (25K and 50K cells) over the course of seven days. All images taken at 3.2x magnification.

	Spheroid Cell Number per 20μL Suspension Volume	
Day	25K	50K
1		
3		
5		
7		

The images were analyzed in ImageJ to determine the diameter of each spheroid on each respective day. The average of each of the three spheroids in each cell density group was taken and plotted against the length of time the spheres were seeded in the hanging drops (Fig. 5.1).

Fig. 5.1. 25K, 50K MDA-MB-231 Spheroid Average Diameter vs Time: Graphical representation of average diameters of all hanging drop spheroids over the course of seven days. Blue bars represent spheroids with 25K cells, while red bars represent spheroids with 50K cells. Diameter is measured in millimeters.

The diameters steadily decreased as the spheroids continued to condense and the days progressed. For the 25K cell group, the average diameter began at approximately 2.81mm on day one. Days two, three, four and five had average diameters of 1.28mm, 1.18mm, 1.00mm, and 0.85mm, respectively. On days six and seven, the average diameters began to plateau. Day six yielded an average diameter of 0.75mm, while day seven yielded an average diameter of 0.69mm.

A similar pattern of exponential decrease can be seen in the average diameters of the 50K cell spheroids. Their maximum average diameter of 3.25mm is seen on day one. From days 2 to 5, the average diameters decreased from 1.70mm to 1.11mm. This cell density group also reached a plateau at days six and seven, resulting in average diameters of 1.06mm and 0.97mm, respectively.

A statistical comparison of diameters of 25K vs 50K cell spheroids was conducted. The result of a double tailed t-test was a p-value of 0.00007392067736, in this case $P = 0.5 > 0.00007392067736$. This value shows that there is no statistically significant difference between the average diameters of the 25K and 50K cell spheroids. However, for our purposes, an evaluation of spheroid morphology, rather than spheroid diameter, was most important in determining which cell density would be best for use within a tissue ring.

5.1.3 Additional Spheroid Observations

Throughout our spheroid experimentation, we made a few additional observations which informed our methodology and working knowledge of these cells in self-aggregation conditions.

The pictures below (Fig. 5.2) show how the drop of media shape affects spheroid formation. Drops that did not have a uniform round shape, resulted in spheroids with elongated projections or otherwise take the general shape of the media droplet. This could be a result of pipette technique when placing drops, movement of drops when flipping the culture plate lid, or jostling movement during transport.

5 mm
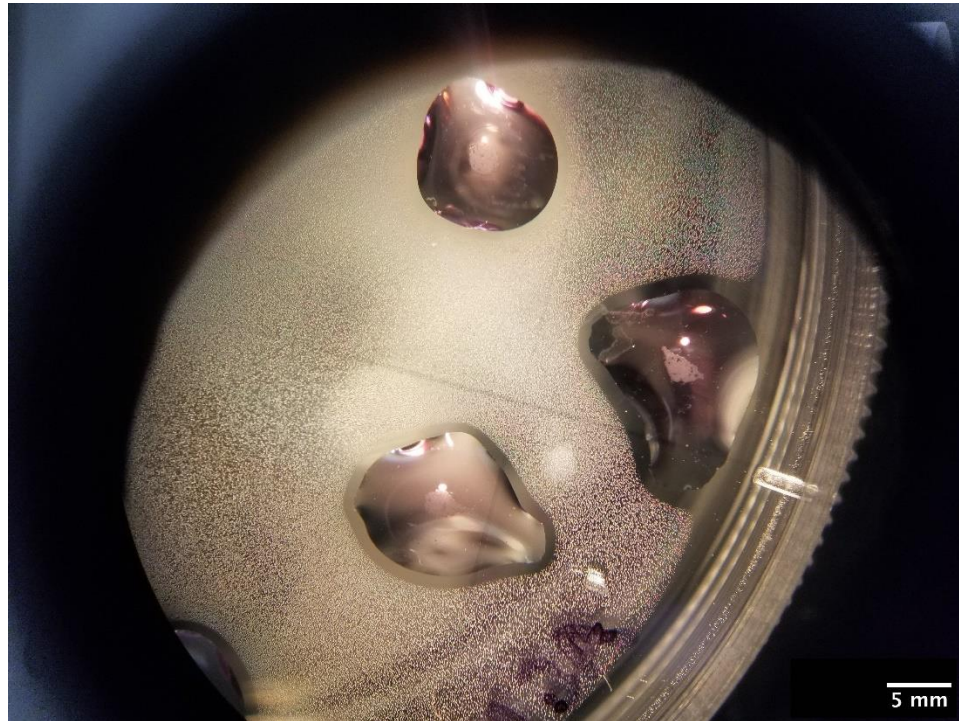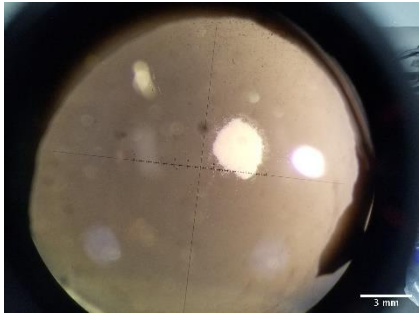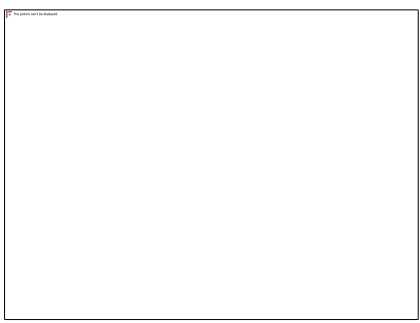
Fig. 5.2. MDA-MB-231 Irregular Cell Aggregation Shape: Through microscopy, we can observe that minute variations in cell suspension drop shape influences the shape of the resultant cell aggregation.

At this stage, we also wanted to test the self-aggregation capacity of the HMF-52 fibroblast cells. We formed fibroblast cell spheroids of 50K cells in 20µL drops. This density was chosen in order to make comparisons to the MDA-MB-231 50K cell spheroid formations. After ten days in hanging drops, we compared the HMF-52 and MDA-MB-231 spheroids and noticed the spheroids appeared to have offshoots of cells and ECM that were not present during initial microscopy (Table 5.3). Because the drops were past the seven-day mark, they had already fully condensed, so the outer portions are not cells and materials that still need to further condense over time. In comparing the two spheroid types, the HMF-52 spheroids appear to have a greater amount of and more visible external material. This could be explained by the fibroblast function of producing ECM, or it could be a biproduct of pipette movement during drop formation.

Table 5.3. Material Surrounding 50K Cell Spheroids: In comparing HMF-52 spheroids to MDA-MB-231 spheroids, there is a significant amount of material generated around and outside of the fibroblast spheroids.

HMF-52 5x Mag	
MDA-MB-231 5x Mag	

Following our MDA-MB-231 spheroid experimentation, we moved on to HMF-52 ring formation trials.

5.2 Cell Suspension Seeded in Rings

Following the development of hanging drops, the team moved on to verify ring aggregation. This was accomplished by 3D printing a negative mold to shape the agarose. The 3D mold was developed in CAD and can be seen in chapter 4.5, Final Design. The result of the punch leaves 4 uniform rings in each well of the 24 well plate, each with a 2mm diameter post in the center of the ring. Following the complete setting of the agarose molds, cells can be seeded into the rings (see Appendix C for full protocol).

HMF-52 cells were seeded in the agarose molds at 120K and 180K cells in each ring, to observe differences in ring formation at different cell concentrations. The 120K cell rings we seeded with 10µL cell suspension. The 180K cell rings were seeded with 15µL cell suspension. These ring structures were left to settle overnight, to allow the cells to self-aggregate and bind to each other through cell-to-cell interactions. The following day, media was gently added to each well of the 24-well plate after the cell suspension settled into the ring wells to reduce risk of disturbing the cells within each ring. These rings were left to culture and analyzed. Images of these cell concentrations were captured using both a cell phone camera and DFK 41BU02 microscope camera and analyzed with IC Capture 2.5 and ImageJ software.

Respective images of different trials were chosen; many images were not clear or showed defined rings due to light refraction through the pink agarose gel. Figure 5.3 shows an HMF-52

ring that contains 180K cells, seeded at a volume of 15µl. We can observe a uniform tissue ring with even distribution of cells throughout.

Fig. 5.3. 180K Fibroblast Cell Ring, 15uL Seeding Volume After 1 Day: One day after seeding 180K cells in 15µL, a tissue ring can be seen within the agarose ring well. Image taken at 3.2x magnification.

After two days in the ring mold, the 180K cell ring remained uniform (Fig. 5.4). In addition to the tissue ring, we can observe ridges in the agarose gel well. Based on the image, it is hard to discern whether cells have attached to the ridges in the gel.

Fig. 5.4. 180K Fibroblast Cell Ring, 15µL Seeding Volume After 2 Days: Two days after seeding 180K cells in 15µL, a tissue ring can be seen within the agarose ring well. Between the tissue ring, seen as a cloudy mass, and the center post, ridges in the agarose gel are visible. Image taken at 3.2x magnification.

The HMF-52 cell rings seeded at a density of 180K cells/15µL were overall uniform and consistent. This uniformity remained over the course of three days. Rings seeded at a density of 120K cells/10µL, did show complete ring formation in the first two days after seeding, but were not as uniform (Fig. 5.6). Ridges in the agarose gel can be seen in this image as well. Dark splotches along these ridges may suggest that cells settled and attached to the agarose in these places outside of the main tissue ring.
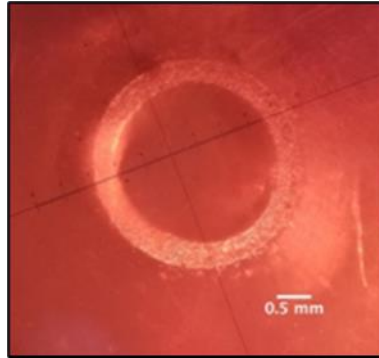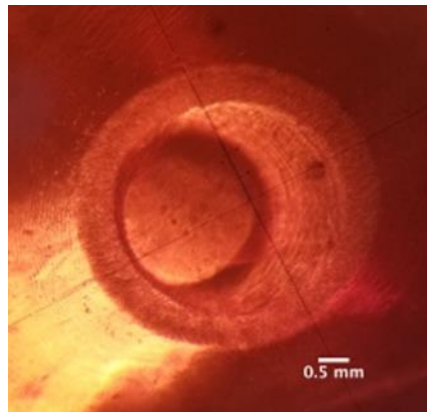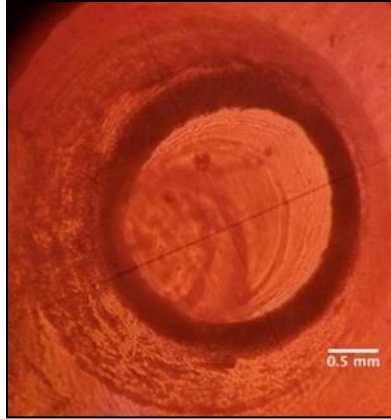
Figure 5.5. 120K Fibroblast Cell Ring, 10µL Seeding Volume After 2 Days: Two days after seeding 120K cells in 10µL, a tissue ring can be seen within the agarose ring well. Besides the dark ring of the main tissue, other cells can be seen clinging to the slanted walls of the gel well. Image taken at 3.2x magnification.

Upon a third day of observation, the 120K HMF-52 cell ring deteriorated (Fig. 5.6). The remaining clusters of cells remained in the ring well, but a contiguous tissue ring was no longer present.
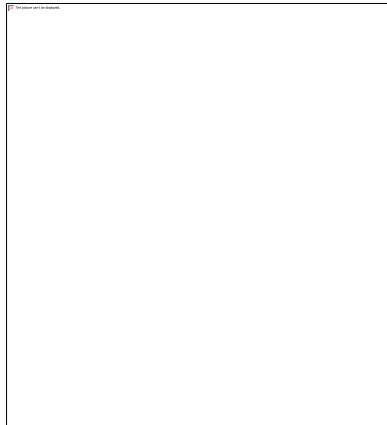
Fig. 5.6. 120K Fibroblast Cell Ring, 10µL Seeding Volume After 3 Days: This image shows the deterioration of a 120K cell fibroblast ring 3 days after being seeded. This image is taken at 3.2x.

In comparing each group of rings, the 180K cells in 15µL seeding volume were the most consistent in forming ring structures. The higher cell number resulted in more uniform tissue rings, with a defined edge and even cell density throughout. The 120K cells in 10µL seeding density did not show this save level of uniformity.

In continued tissue ring observation experiments, prominent abnormalities were noted. These rings were left in the ring molds for an extended period of time. After sixteen days, a 120K cells in 10µL ring had burst (Fig. 5.7, left). This ring was formerly whole, but what can be seen after this extended time were cell clusters distributed within the gel ring well. On this same day, the 180K fibroblast cell rings seeded in 15µL suspension volume appeared to remain as continuous rings. We attempted to extract these remaining rings from the agarose gel, however,

they were extremely fragile. After an unsuccessful attempt, an image was taken that shows where the small hook for ring extraction broke through the tissue ring (Fig. 5.7, right). These rings were deemed far too fragile to remove from the agarose gel wells.
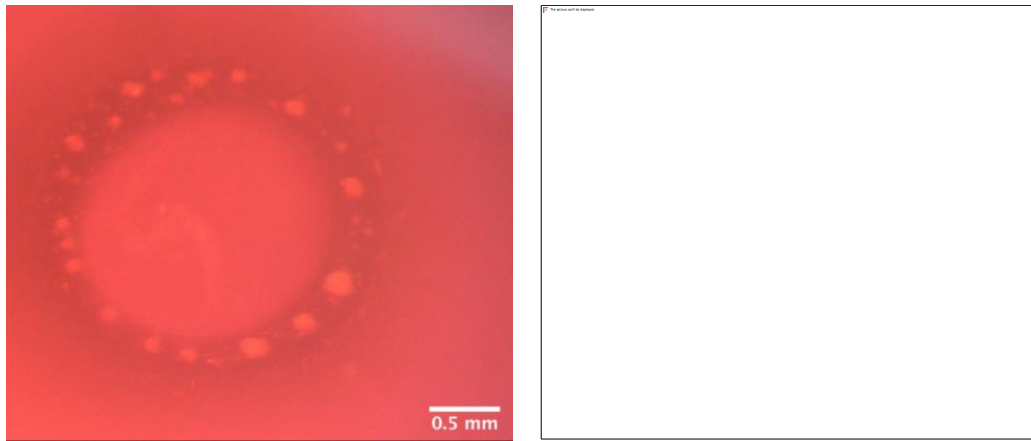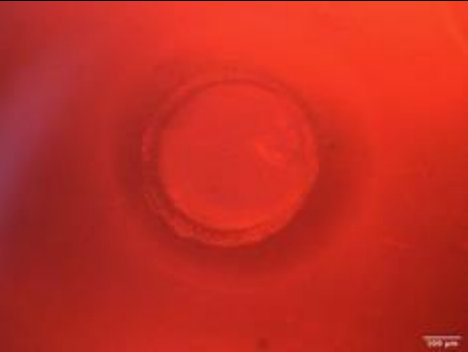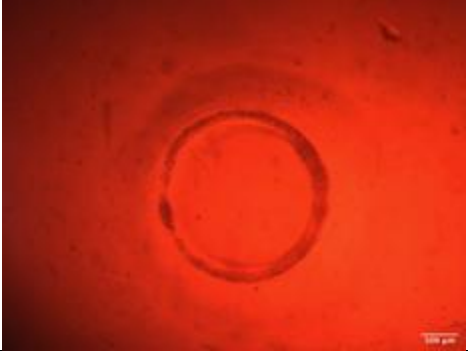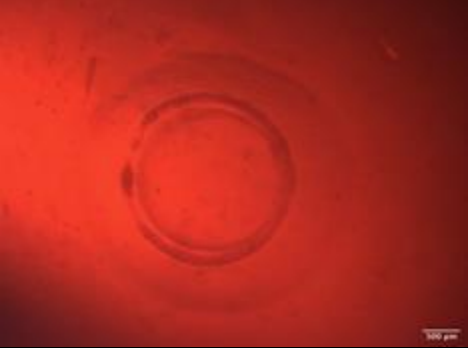
Fig. 5.7. Abnormal Fibroblast Rings: On the left, a ring containing 120K HMF-52 cells within 10µL of volume that burst after 16 days in the ring well. On the right, a ring containing 180K HMF-52 cells within 10µL of volume that remained in the ring mold for 16days. Along the top part of the ring, a section of tissue is missing as a result of trying to extract the ring from the gel.

After these preliminary tests of HMF-52 cell self-aggregation into rings, it was determined that a larger number of cells would be seeded into each ring in future experimentation. Moving forward in our objective to create a combination cancer and fibroblast cell ring, we began our trials of co-culture spheroid and suspension rings.

5.3 Co-Culture Rings – Cell Spheroid Seeding in Ring

While we were culturing the suspension rings of co-cultured HMF-52 and MDA-MB-231, we concurrently cultured an HMF-52 ring structure with a MDA-MB-231 cell spheroid, which were also imaged over the course of four days (Table 5.4). These rings were seeded with $2x10^5$ HMF-52 cells with a $2.5x10^4$ MDA-MB-231 cells spheroid. This was accomplished by spinning down the HMF-52 cells and resuspending in a concentration of $2x10^7$ cells/mL and adding a $2.5x10^4$ MDA-MB-231 cell spheroid. This mixture was put in the premade ring wells in the agarose.

Table 5.4. HMF-52 Cell Suspension with MDA-MB-231 Cell Spheroid Co-Culture Ring Images: Progress images of integrated spheroid rings over four days. Each ring contained 10µL of HMF-52 cell suspension with 200K cell and a single 50K MDA-MB-231 cell spheroid. All images taken at 3.2x magnification.

	HMF-52 Suspension + MDA-MB-231 Spheroid Rings	
Day 1		
Day 2		
Day 3		
Day 4		

Due to time constraints, we used the 2.5×10^4 MDA-MB-231 cells spheroids that were 10 days old. This is close to the end of life for these spheroids, and they did not aggregate as well as we hoped they would. The ring structure with the spheroid was cultured for 4 days and after
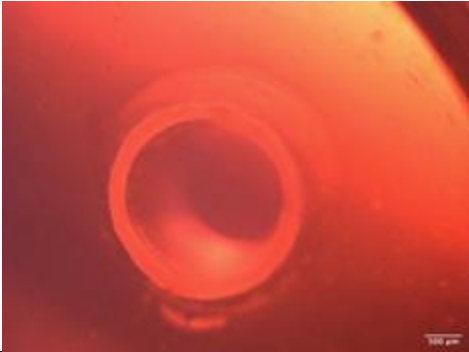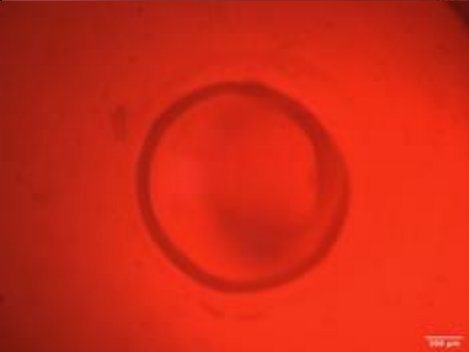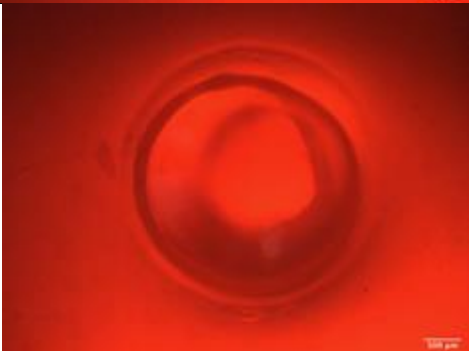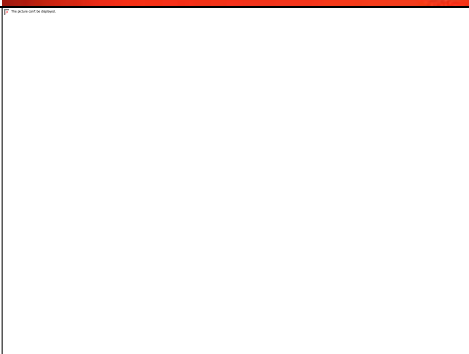
those days in culture we tried to remove the rings from the agarose. Because the rings did not form well, the rings did not move up the center post, which made it difficult to remove the rings intact. In the end, all of the spheroid seeded rings broke apart before they could be imaged with the fluorescent microscope. It was not until after these rings were destroyed that we realized the rings could be imaged while still in the agarose.

5.4 Co-Culture Rings – Cell Suspension Mixture

Continuing our experimentation, we moved on to creating a co-culture of the HMF-52 cells and the MDA-MB-231 cells in a ring structure and observed them for four days (Table 5.5). These rings were seeded with $2x10^5$ HMF-52 cells in a suspension mixture of $2x10^3$ MDA-MB-231 cells. This was accomplished by spinning down the HMF-52 cells and resuspending in a concentration of $2x10^7$ cells/mL and a concentration of $2x10^6$ cells/mL. 10µL of the HMF-52 cell suspension was combined with 1µL of MDA-MB-231 cell suspension. The 11µL mixture was placed in the preformed rings made of agarose.

Due to time constraints, we had to use cells that were at the end of their lives so they did not aggregate as well as it could have with newer cells. Fortunately, they still aggregated, and we could see the self-assembled rings. After 5 days, we decided the rings were formed and we should remove them for imaging. We figured we would see better results with the rings removed, unfortunately, the cells did not move up the middle post in the wells. This made removal of the rings difficult because they are delicate, and we did not want to destroy them. To combat this issue, we opted to image inside of the agarose molds rather than trying to remove the tissue rings.
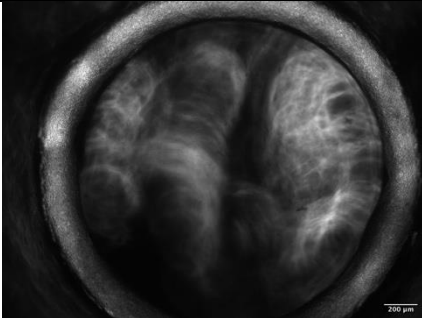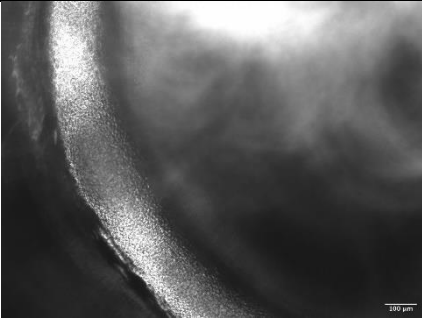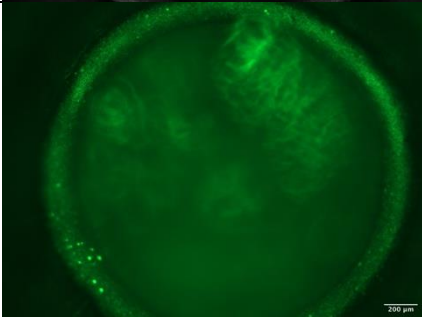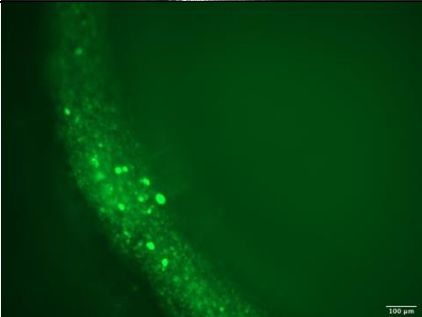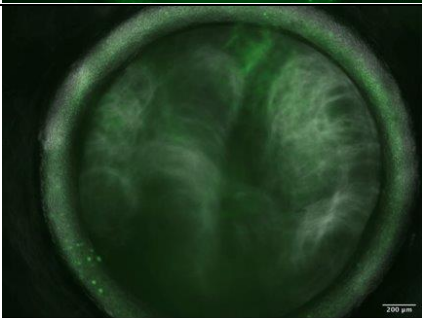
Table 5.5. HMF-52 and MDA-MB-231 Mixed Cell Suspension Ring Images: Progress images of co-culture rings over four days. Each ring had 10μL of 200K HMF-52 cells with 2K MDA-MB-231 cells. All images taken at 3.2x magnification.

	HMF-52 + MDA-MB-231 Mixed Suspension Rings	
Day 1		
Day 2		
Day 3		
Day 4		

The imaging within the agarose molds was completed in Salisbury Labs using a Zeiss Axiovert microscope and camera located in lab 219. These images were exported to the Zeiss

Zen software on a computer and then to ImageJ for further analysis. Our team was able to capture both brightfield and UV excited GFP expressing images. We analyzed the images individually and then overlayed the images to investigate the existence of microtumors within the ring formations (Table 5.6). This analysis revealed the following images. We postulated that the clumps of GFP positive MDA-MB-231 cells are microtumors within the HMF-52 cell rings.

Table 5.6. Phase, GFP, and Overlayed Co-Culture Suspension Ring Images: Phase, GFP and overlayed images of a mixed cell suspension ring at 5x and 10x magnification.

	5x Magnification	10x Magnification
Phase Imaging		
GFP Imaging		
Overlayed Phase/GFP		

Based on our experimentation and observations, we were able to note key phenomena over the course of ring model development. In the next chapter, these results are discussed in further detail, including limitations of our studies and key findings.

6.0 Final Design and Considerations

This chapter details the final design components and methodology. Further design considerations and impacts are also discussed.

6.1 Final Design

Our ring model has the potential to be used as an accurate *in vitro* 3D tumor model to help with personalized cancer therapy testing. To use this model, a biopsy of a solid tumor should be taken from each patient with their specific cancer type along with that patient's own fibroblast cells. A co-culture of cancer cells and fibroblast cells will be used to form the tissue rings within the agarose ring wells created by the 3D printed punch. Following our protocols outlined in the appendices, the co-culture can be seeded into the ring wells either through a cell suspension or inclusion of cancer cell spheroids. Once the tissue ring has been formed and extracted from the agarose gel, the researchers will be able to verify microtumor formation and function and begin cancer treatment testing on these tissue ring models.

6.1.1 Final Design Standards

Some of the potential design standards that we were aiming to meet with our design were outlined in Chapter 3.3. One standard our tumor model would be regulated through is ISO 13845:2016. During the manufacturing process of our ring punch and creation of our cancer model, each step must be monitored for quality. ISO 11737-2:2009 was also met through our sterile cell culture practices, and the use of isopropanol on our ring punch. Further considerations can be made into autoclaving the ring punch, but we had no signs of contamination throughout our model creation process. ISO 20916:2019 is more specific to our *in vitro* tumor model. It will be highly considered during clinical studies of our tumor model to ensure data and subject integrity.

Other standards considered were those of GCCP and the FDA. Throughout our design and testing processes, we maintained standards of GCCP by utilizing sterile and safe cell culture practices and acknowledge that these must be maintained throughout the manufacturing process and further testing in the future. In order to have our tumor model approved for clinical use, it must go through the FDA. Even though it is an *in vitro* tumor model, it is still considered a medical device, especially with the patient specificity. The FDA must approve of our model before it can benefit cancer patients.

6.2 Design Considerations

Along with developing our final design and methodology, external factors and impacts must also be considered. Ranging from economics, political impact, to sustainability and more, we evaluated the ramifications of our design.

6.2.1 Economics

Those who are being treated for cancer have many continuous hospital bills, especially in the cases where the cancer does not have a specified drug therapy. Our proposed tumor model can alleviate some of costs that the patient could face as a result of multiple courses of treatment, combination treatments, or recurring cancer. Our model for treatment testing intends to alleviate some of these costs by treating the patient with the optimal cancer therapy starting with the first administration. By utilizing the most promising treatment to begin with, there could be a

reduction in costs for supplementary or prolonged treatment programs. Also, utilizing a treatment that was previously tested and does minimal damage to the patient's healthy tissues could also save the patient additional costs for care that must be taken to reduce common side effects of treatment. While the economy of everyday living may not be directly affected, those involved in the cancer drug and therapy market will be impacted.

6.2.2 Environmental Impact

With the creation of a patient specific *in vitro* tumor model, there are both positive and negative environmental impacts. Patient specific cell usage will require proper disposal of all biohazardous wastes. The well plates, pipettes, and other culture materials and plastics will also need to be disposed of, oftentimes after just one use, resulting in a large amount of waste. Because many of these materials are classified as biohazards, recycling and reusing methods are not widely available at this time. While our project will use many single-use plastics and other items, there is potentially less wasted because treatments are being trialed on a small-scale rather than on the patient themselves. Trials on patients require other types of single-use items, such as IV needles, bags, and tubing, along with any other equipment needed for the hospital stay. Our *in vitro* tumor model does not require the patient to remain in the hospital for treatment trials, thus eliminating patient waste.

6.2.3 Societal Influence

Our *in vitro* tumor model has the potential to revolutionize cancer therapies. As specified in the economics section above, the cost to the patient can be minimized through the high throughput testing of various therapies on a small-scale, allowing for smaller amounts of drugs and supplies to be needed. This cut in cancer patient costs opens opportunities for more people in the middle and lower socioeconomic classes to have access to cancer treatments that would have previously been unaffordable. The cancer community could have more survivors with more treatment options and our tumor model would help make a cancer diagnosis less grim. Our *in* vitro tumor model creates a new pathway for doctors and researchers in personalized medicine.

6.2.4 Political Ramifications

Our *in vitro* tumor model has the potential to make a big impact in the cancer therapy market. Companies that produce the different cancer drugs make a large profit from patients that have to go through multiple trials and therapies. With the creation of our model, less drug will be needed for each trial, however, more people will have access to multiple treatment options. There is not likely to be a large change in the profitability of the drug companies because the small-scale aspect will be balanced out by the more expansive patient network. Because these drug companies are global, the use of our tumor model will cause a momentary shift in the global cancer drug market.

When looking at the impact our *in vitro* tumor model on other countries, there will be differences based on the medical systems in place. There will be similar benefits that can be realized from our model in countries with similar healthcare systems to the United States, but our small-scale model has the potential to create new benefits in countries with less funding and access to cancer therapies. As stated above, less drug and materials are needed along with fewer patient trials, thereby cutting costs. In countries with less wealth and funding, our model has the potential to allow access to more variation in cancer therapies in other countries due to the lesser

price, which in turn would also provide a brighter outlook for cancer patients within those countries.

6.2.5 Ethical Concerns

While the field of personalized medicine has continued to grow for more than a decade, so have the ethical implications of this research. Since it is still an up-and-coming field of study, there are many ethical concerns. Privacy is an increasing concern especially with electronic health records (EHRs) that can contain decades worth of previous medical history [47]. This and other sensitive information can be viewed by anyone who has access to a patient's EHR. This leads to questions regarding patient and physician confidentiality and how much information the researchers conducting these treatments would have access to.

Personalized medicine also has an increased risk of error by a healthcare provider due to its complexity [47]. A medical error creates the potential for liability but figuring who would be liable is where there is concern. A patient's physician may be responsible for their overall care; however, they are not typically experienced in the field of personalized medicine. Especially since it is still a growing industry. Several parties could also be at fault, including the testing laboratories, the medical device manufacturers, the researchers, pharmaceutical companies, and more. Physicians and other parties could also be liable for unwanted release of sensitive medical information that come with EHRs mentioned earlier. This leads to additional legal responsibilities that come with the advancement of personalized medicine.

6.2.6 Health and Safety Issues

Our proposed tumor model has the potential to improve the field of cancer treatment and increase the rate of survival. This model will allow doctors and researchers to find the most effective treatment method for each individual patient by eliminating treatments that would be ineffective. This process removes the overall number of treatments and limits the side effects that the patient must endure. Our main concern with this method of treatment is that it could be a very time-consuming process. Patients in later stages of cancer may not have the time to wait for the proper research to be conducted and may be forced to proceed with traditional treatment methods. This could limit the population that could benefit from our model.

6.2.7 Manufacturability

Methods used to create the 3D tumor model were relatively simple and could be easily replicated. Small scale testing could be done on tumor models in any research lab, while larger scale testing may need to be done in outside testing facilities. The 3D printed tissue ring model used to create the agarose mold cost around $2 to manufacture with durable resin and a glossy finish. This could be made with any Form Labs 2 Form 2 model 3D printer and could easily be altered for large scale production. The tissue samples and biopsies may be the hardest material to obtain during this process because they must come from each individual patient.

The protocols used to form the hanging drop spheroids and create the agarose ring molds can be found in Appendix B and Appendix C, respectively. Protocols for creating the tissue rings in a 3D culture can be found in Appendix D, and protocols for our fibroblast and MDA-MB-231 co-culture can be found in Appendix E and Appendix F.

6.2.8 Sustainability

Since our tumor model is specific to each patient, a new model would need to be used for each patient and for each treatment method. However, our device is not creating a new type of waste that has not been dealt with before. All materials used to manufacture the model, maintain the cell cultures and biopsies, and maintain the model are disposed of through biohazard waste. Biohazard waste can be found in almost all research laboratories, so it does not require a separate method of disposal. There is no way for our model to be completely sustainable but there should always be biohazard waste bins present when working with or making our device.

7.0 Discussion

The results from our project show great potential for using ring formations as *in vitro* cancer models. Our experiments with hanging drop spheroid formation, HMF-52 ring formation, and co-culture ring formation helped us to accomplish and better understand our objectives. With our final experimentation being the co-culture of HMF-52 cells and MDA-MB-231 cells in a ring mold, we needed to better understand each aspect that would go into the co-culture before we put it all together. COVID-19 lab restrictions early in the year set our experimenting time frame back extensively, causing a significant decrease in trials and variety of experiments performed. We also had significant trouble after our primary cell line of HMF-52 cells reached senescence at a key time during our ring formation experiments. With these setbacks taken into consideration, our preliminary findings can be built upon in later project iterations to form a more significant dataset, and more precise conclusions.

The hanging drop experimentation was the first experiment we ran, and it yielded spheroid formation regardless of the number of cells we seeded in each drop, showing that both HMF-52 cells and MDA-MB-231 cells were capable of self-aggregation and that a scaffold-less 3D model was a viable option. This experimentation allowed us to observe the conditions that were best for a strong and uniform spheroid. Our first trial with the range in seeding from 20K to 240K cells per drop led us to observe that the 50K cell spheroids were most uniform, which includes an even, round edge, and consistent cell density across the sphere. The spheroids with fewer cells were not as uniform and had cell clusters that were not part of the main spheroid and holes throughout. The porous appearance of the 20K cell spheroids were not as uniform as the 50K cell spheroids, however, the porous spheroids may be beneficial for use in a 3D model because they allow for greater nutrient exchange with the surrounding cell environment and could be beneficial for spheroid integration into a surrounding tissue. A downside of the non-uniformity could be that the strength and overall integrity of the spheroid could be compromised and may break apart during any type of transfer or manipulation. On the larger end of our trials, the 120K and 240K cell spheroids were far too large and did not make a uniform, condensed spheroid. From our trials, 120K was the upper limit of cells per drop. For all seeding concentrations, we observed changes in spheroid shape depending on drop shape, showing that the cells aggregate according to the confines of the structure they are cultured in.

Following the initial hanging drop experimentation, our week-long trial of drops containing 25K and 50K MDA-MB-231 cells helped us determine when the drops would be ready to be transferred into a ring well for integration into a ring tissue. We shifted our spheroid formation to only MDA-MB-231 cells because placing these spheroids within our ring molds would represent the tumors and CTC clusters found in cancer patients. Our results showed that both the 25K and 50K cells per drop were viable options for ring seeding, but due to poor cell proliferation in culture, we determined that we would create 25K cells per spheroid for future trials. Both densities compacted and aggregated into spheroids throughout the 7 day study, and we were able to measure their diameters using ImageJ to quantitatively compare differences in diameter. Because our ring molds were small, we needed to ensure that the spheroids would be able to fit within the ring well. Additionally, we noticed that the diameter changes plateaued around day 5, so we determined that the best day to transfer the spheroids from the hanging drops into the ring wells would be day 6 or 7. Any additional time following day 7 would result in weak spheroids that broke up when moved. In attempts to move 12-day old spheroids into the ring wells, the spheroids broke up during transfer because of the age of the cells, inability to

replenish with new culture media, and their weakened cell-to-cell interactions over time. This supports the 7 days limit for keeping the spheroids in their hanging drops.

Once the team verified the best conditions for the spheroid hanging drops, tissue ring formation was trialed. Before we could seed cells, various iterations of our punch prototype were used to create the agarose ring wells. We used 2% w/v molten agarose in a 24-well plate and found that 1.6mL of molten agarose provided the best ring well depth in the gel. These ring wells were deep enough to hold a maximum of 7μL of cell suspension, while still being shallow enough to be able to image and access the rings once they had formed. The final 3D printed ring punch was comprised of white durable resin with a glossy finish. The smooth surface provided by the glossy finish was key for forming optimal ring wells. Previous iterations of the punch without glossy finish resulted in rings wells with a rough surface. Although cells typically do not adhere to agarose, the surface roughness allowed for cells to stick to the sides of each well, rather than aggregate together at the bottom of the well to form rings. The punches can be sprayed and wiped with 70% isopropanol to be sterilized in accordance with GCCP. Once the punches were sterilized, they were covered and left in the biosafety cabinet so that they would not be broken down by repeat alcohol exposure. While alcohol sterilization is not the best method for cell culture, we were unable to perform testing on other possible sterilization techniques due to time constraints.

Following the formation of the agarose gel molds, we conducted trials to see how the cells would aggregate in the ring wells. The seedings of 120K and 180K HMF-52 cells showed successful tissue creation in the ring shape, but we would need to use more cells in order to reliably grow a complete tissue ring. These trials confirmed the ability of HMF-52 cells to self-aggregate. These experiments were more rudimentary, and along with suggestions from previous ring model work, we knew that we wanted to seed at least 300K cells per ring. Over the course of these trials, we were also able to evaluate our 3D printed ring well punch. Using initial protypes, ridges can be seen along the sides of the ring wells (Fig. 5.4 and Fig. 5.5). The ridges we saw in these agarose rings were due to the material and printing quality of some of the punch parts we produced. These ridges hindered tissue ring formation because rather than adhere to each other, the cells attached to the agarose gel. In order to minimize the roughness of the wells, multiple iterations of the punch were printed to achieve the smoothest surface possible.

Before the end of this project, we wanted to experiment with our HMF-52 and MDA-MB-231 co-culture idea. Unfortunately, our HMF-52 cells started senescing and our MDA-MB-231 cells stopped proliferating as rapidly. We were only able to seed four rings of the suspension co-culture and the MDA-MB-231 spheroid co-culture with only 200K cells, and our fluorescence imaging only provided results for two of the suspension co-culture rings. This was due to our team not having an established ring removal technique and the fact that we had to use older cells and spheroids, so they did not aggregate into sturdy rings as we were expecting.

Apart from these limitations, the fluorescence imaging of our MDA-MB-231 and HMF-52 suspension co-culture rings lead us to believe that MDA-MB-231 microtumors were formed within the contiguous structure of the HMF-52 fibroblast ring. When the phase images were overlayed on the GFP filtered image, we saw that each GFP positive site was comprised of a clump of cells and was not just one cell with a strong fluorescence. These microtumors completely self-aggregated without the help of an initial cluster forming technique before integration within the ring. Because only two rings were able to be analyzed through fluorescence microscopy, we understand that no statistically significant assumptions can be

made. However, we do think that this potential formation of microtumors gives the future project groups a good basis to work from.

It is difficult to compare our model's experimentation results to different outcomes of cancer models in use today because our findings are very preliminary. With that being said, our model does and has the potential to address many problems with the current models. The ring structure gives a contiguous structure for cancer microtumors to grow within, and because there is no scaffold, the cell-to-cell interactions are not hindered. While we were not able to carry out further tests, we believe that our model has the potential to be used to monitor metastasis and can be used with patient specific cell types. One of the biggest successes of our model is that the co-culture aspect allows for drugs to be tested on both cancerous and non-cancerous tissues simultaneously. The normal fibroblast tissue grows in a similar structure to *in vivo* states so the effect of the cancer drugs can be monitored accordingly.

Overall, the biggest limitation to our results was restricted lab access and time due to the COVID-19 pandemic. Due to this, experiments had to be run with less than ideal cell numbers and trials. Because of this, we hope that future project groups can produce more trials of our experiments and look more into assays involving metastasis and drug penetration. In the end, we were able to accomplish our objectives of successful cell culture and proliferation of cancerous and non-cancerous cells, along with the manipulation of cell formation into 3D shapes when we ran trials of spheroids and tissue ring formation. Our third objective of monitoring metastasis was only half met with the observation of microtumors within the co-cultured rings. We were not able to obtain any data on time of metastasis, or to what extent, but we know that the cancerous cells were incorporated throughout the fibroblast structure. We were not able to meet our last objective of assessing our model's accuracy to the *in vivo* tumor environment or patient specific modeling, but we do believe that this can be accomplished in future works.

8.0 Conclusions and Recommendations

Based on our trials and results, we can draw a handful of conclusions on best practices and techniques for 3D microtumor tissue ring formation.

8.1 Conclusions

Based on the team's results and experimentation, our 3D printed punch and methods for creating agarose ring wells were easily replicable and produced a high success rate. These molds created 4 uniform rings within each well of a 24 well plate, along with a center post that allowed cells to be seeded into ring structures. Our design also has the potential to be patient specific, utilizing the patient's own fibroblast and tumor cells in order to create their own personalized tissue tumor model. Lastly, after further experimentation and development, this model has the potential to accurately model the *in vivo* tumor state. Based off the Final Design Matrix, Table 4.2, our ring model showed the greatest potential to produce accurate models of the *in vivo* tumor state compared to other design concepts. This could result in future use in cancer therapy screening.

8.2 Recommendations

For future iterations of this project and continued development in this field of research, we have multiple recommendations. These recommendations address areas of experimentation we were not able to conduct ourselves as well as recommendations to broaden the scope of this project.

8.2.1 Removal of Tissue Rings

Further research needs to be conducted in order to develop a standardized technique for removing the tissue rings from the agarose well molds. Even though a protocol was established to create successful agarose molds, the team was unable to finalize an effective method for removing the tissue rings from the mold. It will be important to be precise when trying to remove the tissue rings from the agarose gel because the tissue is fragile. A standardized method of ring removal, either by extracting the tissue rings from the mold or by peeling the agarose away from the tissue ring or any other method, will be essential in being able to analyze, image, and test the ring formations. For ease of tissue ring removal, we recommend an extremely smooth punch for agarose gel ring well creation. Any roughness of the ring well resulting from any surface defects or texture of the punch will impact the cell self-aggregation. A completely smooth ring well will force the cells to aggregate to each other, rather than adhere to the walls of the ring well. Limiting adherence to the agarose is key for ring removal.

Once the rings are removed from the agarose, they will need to be anchored to something in order to maintain cell health in extended culture. Because these methods work with adherent cell types, they will be the most proliferative and functional if the ring is attached to something. Further tests could determine whether the ring models maintain their structure depending on various anchored vs non-anchored conditions. The attachment of the ring to a secondary surface would have numerous aspects to be considered in order to ensure that the ring model will still be able to serve its purpose as a way to test cancer treatments, while also being accurate to the *in vivo* state.

8.2.2 Fibroblast to Cancer Cell Ratio

Additionally, the proper fibroblasts to tumor cell ratio should be determined in order to create accurate microtumors. While the team was able to see some microtumors or cluster of cells through GFP imaging (see Chapter 5.3), the team was unable to run multiple trials with different cell ratios to determine if one provided more consistent microtumors. Testing this ratio should involve extensive monitoring of cancer cell or microtumor integration into the surrounding fibroblasts. For more accurate cell-to-cell interactions, it is important that the cancer cells are able to survive, proliferate, migrate, etc., within the fibroblast ring. Further research can also be performed into the amount of cancerous tissue in relation to normal tissue in cancer patients. This ratio can also be modified on a patient-to-patient basis.

8.2.3 Ring Formation with Various Cell Types

We also believe further experimentation should be conducted to use different cell types to create tissue rings and see how they compare. Various cancer types should be experimented with in order to ensure this model's efficacy for each type. Our project only worked with breast cancer cells, but we predict that, due to the proliferative behaviors of cancer cells, that other cancer types would work as well. However, it is important to note that this model will likely only work with solid tumor cells that can create CTCs. Other blood and liquid related cancers are more limited with this approach but can be a consideration for further projects.

8.2.4 Analysis and Enrichment of Microtumor and Tissue Environment

In a research environment with more resources and a longer period of time for development, there would be better access to testing strategies to validate the accuracy of the *in vitro* tumor environment. Various tests should be run on the tissue ring models to validate the function of the different cells within the tissue rings. In addition to tests, proteins, cytokines and chemokines that would typically be found in the cancer tumor microenvironment should be added to the culture to further emulate the *in vivo* state.

Various assays can be performed to ensure that the cancerous cells in the culture are being expressed in the model's microenvironment. These assays can include cytokines, including important signaling cytokines such as TNF-α**,**TGF-β and VEGF [48]. In addition to these, chemokines such as IL-6 and IL-10can be screened for in the model's microenvironment [48]. Other proteins to analyze that could provide insight into cancer cell function within the tissue structure are metalloproteinases. Metalloproteinases are utilized by cancer cells to break down surrounding ECM to clear paths for invasion into surrounding tissues [49]. Screening for metalloproteinase presence and function could validate any invasion or migration of cancer cells throughout the tissue model. In addition to the accuracy to the *in vivo* environment, many cancerous cells use cytokines and chemokines for crosstalk between cells. These assays can give an idea to the team whether or not the cancerous cells and the healthy tissue are communicating in ways they would be *in vivo.*

After running various assays to discover if any and what cytokines, chemokines and proteins are existing in the microenvironment, a team can look at enriching and supplementing the culture. The addition of proteins that would be found in the *in vivo* environment can further increase to the likelihood that screening with different cancer treatments will give an accurate idea how that person's cancer will respond.

We hope these recommendations will assist future projects and research teams in improving upon our design and working towards an accurate 3D tumor model for use in cancer therapy treatment testing. Eventually, we hope to see this model expanded to uses in a clinical setting using circulating tumor cells for early cancer detection and treatment.

References

[1]   A. C. Society, "Global Cancer Facts and Figures 4th Edition," Atlanta, GA, 2018.

[2]   "Cancer Treatment & Survivorship Facts & Figures 2019-2021," 2019. [Online]. Available: https://www.cancer.org/content/dam/cancer-org/research/cancer-facts-and-statistics/cancer-treatment-and-survivorship-facts-and-figures/cancer-treatment-and-survivorship-facts-and-figures-2019-2021.pdf

[3]   M. Arruebo *et al.*, "Assessment of the evolution of cancer treatment therapies," (in eng), *Cancers (Basel),* vol. 3, no. 3, pp. 3279-330, Aug 2011, doi: 10.3390/cancers3033279.

[4]   T. Cheng and X. Zhan, "Pattern recognition for predictive, preventive, and personalized medicine in cancer," *EPMA Journal,* vol. 8, no. 1, pp. 51-60, 2017/03/01 2017, doi: 10.1007/s13167-017-0083-9.

[5]   M. A. Aziz, Z. Yousef, A. M. Saleh, S. Mohammad, and B. Al Knawy, "Towards personalized medicine of colorectal cancer," *Critical Reviews in Oncology/Hematology,* vol. 118, pp. 70-78, 2017/10/01/ 2017, doi: https://doi.org/10.1016/j.critrevonc.2017.08.007.

[6]   N. C. Institute. "What Is Cancer?" National Institute of Health. https://www.cancer.gov/about-cancer/understanding/what-is-cancer#:~:text=Cancer%20is%20the%20name%20given,up%20of%20trillions%20of%20cells (accessed 2020).

[7]   "What is Metastasis?" https://www.cancer.net/navigating-cancer-care/cancer-basics/what-metastasis (accessed 2020).

[8]   N. C. Institute. "Metastatic Cancer." https://www.cancer.gov/types/metastatic-cancer (accessed 2020).

[9]   S. C. P. Williams, "Circulating tumor cells," (in eng), *Proceedings of the National Academy of Sciences of the United States of America,* vol. 110, no. 13, pp. 4861-4861, 2013, doi: 10.1073/pnas.1304186110.

[10]   D. Akolkar *et al.*, "Circulating ensembles of tumor-associated cells: A redoubtable new systemic hallmark of cancer," *International Journal of Cancer,* vol. 146, no. 12, pp. 3485-3494, 2020, doi: 10.1002/ijc.32815.

[11]   A. Gaya *et al.*, "Evaluation of circulating tumor cell clusters for pan-cancer noninvasive diagnostic triaging," *Cancer Cytopathology,* vol. n/a, no. n/a, doi: 10.1002/cncy.22366.

[12]   D. A. Haber and V. E. Velculescu, "Blood-Based Analyses of Cancer: Circulating Tumor Cells and Circulating Tumor DNA," *Cancer Discovery,* vol. 4, no. 6, p. 650, 2014, doi: 10.1158/2159-8290.CD-13-1014.

[13]   "Breast Cancer - Metastatic: Diagnosis." ASCO Journals. https://www.cancer.net/cancer-types/breast-cancer-metastatic/diagnosis (accessed 2020).

[14]   M. E. Menezes *et al.*, "Detecting Tumor Metastases: The Road to Therapy Starts Here," (in eng), *Advances in cancer research,* vol. 132, pp. 1-44, 2016, doi: 10.1016/bs.acr.2016.07.001.

[15]   D. Madhavan *et al.*, "Circulating miRNAs with prognostic value in metastatic breast cancer and for early detection of metastasis," *Carcinogenesis,* vol. 37, no. 5, pp. 461-470, 2016, doi: 10.1093/carcin/bgw008.

[16]   Y. Zhang, Y. Lv, Y. Niu, H. Su, and A. Feng, "Role of Circulating Tumor Cell (CTC) Monitoring in Evaluating Prognosis of Triple-Negative Breast Cancer Patients in China,"

(in eng), *Medical science monitor : international medical journal of experimental and clinical research,* vol. 23, pp. 3071-3079, 2017, doi: 10.12659/msm.902637.

[17]   "Treatment for cancer." https://www.cancerresearchuk.org/about-cancer/cancer-in-general/treatment (accessed 2020).

[18]   M. R. Carvalho, D. Lima, R. L. Reis, V. M. Correlo, and J. M. Oliveira, "Evaluating Biomaterial- and Microfluidic-Based 3D Tumor Models," *Trends in Biotechnology,* vol. 33, no. 11, pp. 667-678, 2015/11/01/ 2015, doi: https://doi.org/10.1016/j.tibtech.2015.09.009.

[19]   M. Kapałczyńska *et al.*, "2D and 3D cell cultures - a comparison of different types of cancer cell cultures," (in eng), *Archives of medical science : AMS,* vol. 14, no. 4, pp. 910-919, 2018, doi: 10.5114/aoms.2016.63743.

[20]   D.-J. Cheon and S. Orsulic, "Mouse Models of Cancer," *Annual Review of Pathology: Mechanisms of Disease,* vol. 6, no. 1, pp. 95-119, 2011/02/28 2011, doi: 10.1146/annurev.pathol.3.121806.154244.

[21]   K. K. Frese and D. A. Tuveson, "Maximizing mouse cancer models," *Nature Reviews Cancer,* vol. 7, no. 9, pp. 654-658, 2007/09/01 2007, doi: 10.1038/nrc2192.

[22]   M. Sepantafar *et al.*, "Engineered Hydrogels in Cancer Therapy and Diagnosis," *Trends in Biotechnology,* vol. 35, no. 11, pp. 1074-1087, 2017/11/01/ 2017, doi: https://doi.org/10.1016/j.tibtech.2017.06.015.

[23]   S. Pradhan, I. Hassani, W. J. Seeto, and E. A. Lipke, "PEG-fibrinogen hydrogels for three-dimensional breast cancer cell culture," *Journal of Biomedical Materials Research Part A,* vol. 105, no. 1, pp. 236-252, 2017/01/01 2017, doi: 10.1002/jbm.a.35899.

[24]   S. Breslin and L. O'Driscoll, "Three-dimensional cell culture: the missing link in drug discovery," *Drug Discovery Today,* vol. 18, no. 5, pp. 240-249, 2013/03/01/ 2013, doi: https://doi.org/10.1016/j.drudis.2012.10.003.

[25]   N. Gupta, J. R. Liu, B. Patel, D. E. Solomon, B. Vaidya, and V. Gupta, "Microfluidics-based 3D cell culture models: Utility in novel drug discovery and delivery research," (in eng), *Bioengineering & translational medicine,* vol. 1, no. 1, pp. 63-81, 2016, doi: 10.1002/btm2.10013.

[26]   E. Fennema, N. Rivron, J. Rouwkema, C. van Blitterswijk, and J. de Boer, "Spheroid culture as a tool for creating 3D complex tissues," *Trends in Biotechnology,* vol. 31, no. 2, pp. 108-115, 2013/02/01/ 2013, doi: https://doi.org/10.1016/j.tibtech.2012.12.003.

[27]   R. Sutherland, J. Carlsson, R. Durand, and e. al., "Spheroids in Cancer Research," *The Journal of Cancer Research,* vol. 41, pp. 2980-2984, 1981.

[28]   A. Navis. "Hanging Drop Tissue Culture." https://embryo.asu.edu/pages/hanging-drop-tissue-culture#:~:text=The%20classic%20hanging%20drop%20culture,from%20an%20inverted%20watch%20glass.&text=This%20allows%20tissues%20or%20other,being%20squashed%20against%20a%20dish (accessed 2020).

[29]   T. Rodrigues *et al.*, "Emerging tumor spheroids technologies for 3D in vitro cancer modeling," *Pharmacology & Therapeutics,* vol. 184, pp. 201-211, 2018/04/01/ 2018, doi: https://doi.org/10.1016/j.pharmthera.2017.10.018.

[30]   J. Friedrich, C. Seidel, R. Ebner, and L. A. Kunz-Schughart, "Spheroid-based drug screen: considerations and practical approach," *Nature Protocols,* vol. 4, no. 3, pp. 309-324, 2009/03/01 2009, doi: 10.1038/nprot.2008.226.

[31]   K. Duval *et al.*, "Modeling Physiological Events in 2D vs. 3D Cell Culture," *Physiology,* vol. 32, pp. 266-277, 2017, doi: 10.1152/physiol.00036.2016.

[32]   A. Y. Hsiao *et al.*, "Micro-ring structures stabilize microdroplets to enable long term spheroid culture in 384 hanging drop array plates," (in eng), *Biomedical microdevices,* vol. 14, no. 2, pp. 313-323, 2012, doi: 10.1007/s10544-011-9608-5.

[33]   !!! INVALID CITATION !!! [28].

[34]   H. Sherman, H. J. Gitschier, and A. E. Rossi, "A Novel Three-Dimensional Immune Oncology Model for High-Throughput Testing of Tumoricidal Activity," (in eng), *Frontiers in immunology,* vol. 9, pp. 857-857, 2018, doi: 10.3389/fimmu.2018.00857.

[35]   K. E. Sung *et al.*, "Transition to invasion in breast cancer: a microfluidic in vitro model enables examination of spatial and temporal effects," (in eng), *Integrative biology : quantitative biosciences from nano to macro,* vol. 3, no. 4, pp. 439-450, 2011, doi: 10.1039/c0ib00063a.

[36]   "Mission." Personalized Medicine Coalition. http://www.personalizedmedicinecoalition.org/ (accessed.

[37]   F. R. Vogenberg, C. Isaacson Barash, and M. Pursel, "Personalized medicine: part 1: evolution and development into theranostics," (in eng), *P & T : a peer-reviewed journal for formulary management,* vol. 35, no. 10, pp. 560-576, 2010.

[38]   "About Us." https://www.iso.org/about-us.html (accessed 2020).

[39]   "ISO 13485." https://www.iso.org/iso-13485-medical-devices.html (accessed 2020).

[40]   "ISO 20916:2019." https://www.iso.org/standard/69455.html (accessed 2020).

[41]   "ISO 11737-2:2009." https://www.iso.org/standard/44955.html (accessed 2020).

[42]   "What We Do." https://www.fda.gov/about-fda/what-we-do (accessed 2020).

[43]   S. Coecke *et al.*, "Guidance on good cell culture practice. a report of the second ECVAM task force on good cell culture practice," (in eng), *Altern Lab Anim,* vol. 33, no. 3, pp. 261-87, Jun 2005, doi: 10.1177/026119290503300313.

[44]   Y. Li and E. Kumacheva, "Hydrogel microenvironments for cancer spheroid growth and drug screening," *Science Advances,* vol. 4, no. 4, p. eaas8998, 2018, doi: 10.1126/sciadv.aas8998.

[45]   H. A. Strobel *et al.*, "Assembly of Tissue-Engineered Blood Vessels with Spatially Controlled Heterogeneities," (in eng), *Tissue engineering. Part A,* vol. 24, no. 19-20, pp. 1492-1503, 2018, doi: 10.1089/ten.TEA.2017.0492.

[46]   J. Forte, "Development of a Biomimetic In Vitro Skeletal Muscle Tissue Model," Ph.D. dissertation, 2017.

Appendix A: Protocol for Sub-Culturing and Passaging of Cells

Adapted from Professor Ambady at Worcester Polytechnic Institute

Purpose: To maintain healthy cells in culture or to expand the number of cells in culture.

Materials:

- Complete Cell Culture Media (CM)
    - DMEM basal media with high glucose, sodium pyruvate, phenol red, sodium bicarbonate, Fetal bovine serum, Glutamax (200mM), and Penicillin/Streptomycin (Penn-Strep) (100X)
- Trypsin (0.25% stock solution; prepare 0.05% working solution)
- Sterile 1X DPBS (-)
- Sterile tubes and culture plates/flasks
- Incubator (5% CO2; 37°C)
- Biological Safety Cabinet (BSC)
- Centrifuge
- Microscope
- Serological pipets
- Motorized pipet aid
- Vacuum trap
- Sterilized Pasteur pipets
- Solvent resistant markers
- Spray bottle containing 70% ethanol
- Kimwipes
- Gloves

Complete Media (CM) Preparation:

For 500 mL CM	Final Concentration	Volume (mL)
Fetal Bovine Serum (FBS)	10%	50
Glutamax (200mM)	1%	5
Penn-Strep (100x)	1%	5
DMEM Basal Media	(up to 500 mL)	440
Total Volume:		**500**

Procedure:

1. Prior to taking the cell plate/flask to the BSC, check the cells under a microscope to ensure cell life with 70-80% confluency and no contamination.
2. Bring cells into sterilized BSC.
3. Aspirate medium using vacuum pump and wash cells twice with 1X DPBS (-) by adding and then aspirating DPBS (-) using a serological pipette.
4. Trypsinize cells by adding 3mL 1X trypsin EDTA for 3-5 mins. Plates may be returned to the incubator or plate warmer while trypsinizing.
    a. After 3-5 mins. check cells under a microscope to ensure detachment.
5. Using a new serological pipette, add 2mL of fresh media to the plate/flask.
    a. Using the serological pipette, break up cells by pipetting up and down back into the plate to remove any stuck cells and break apart cell clumps.
6. Transfer cells in 5mL solution to fresh 15mL conical tube.
    a. If performing a cell count, take a 7µL sample from this solution.

7. Place tube in centrifuge with proper counterbalance, a 15mL conical tube with equal volume of water, for 5 mins. at 200G.
    a. Following centrifuge use, identify the cell pellet.
8. Aspirate excess media surrounding the pellet using the vacuum pump with a fresh Pasteur pipette.
9. Resuspend cells in appropriate amount of media in the conical tube and break up cell pellet by repeat pipetting using a serological pipette. A cell count should be conducted and used to determine desired cell number plating (see below).
10. Plate the appropriate number of cells into a fresh plate and add supplementary media.
    a. Check under microscope to ensure cell transfer.
11. Transfer new plate/flask(s) into incubator for desired amount of time.

Cell Counting:
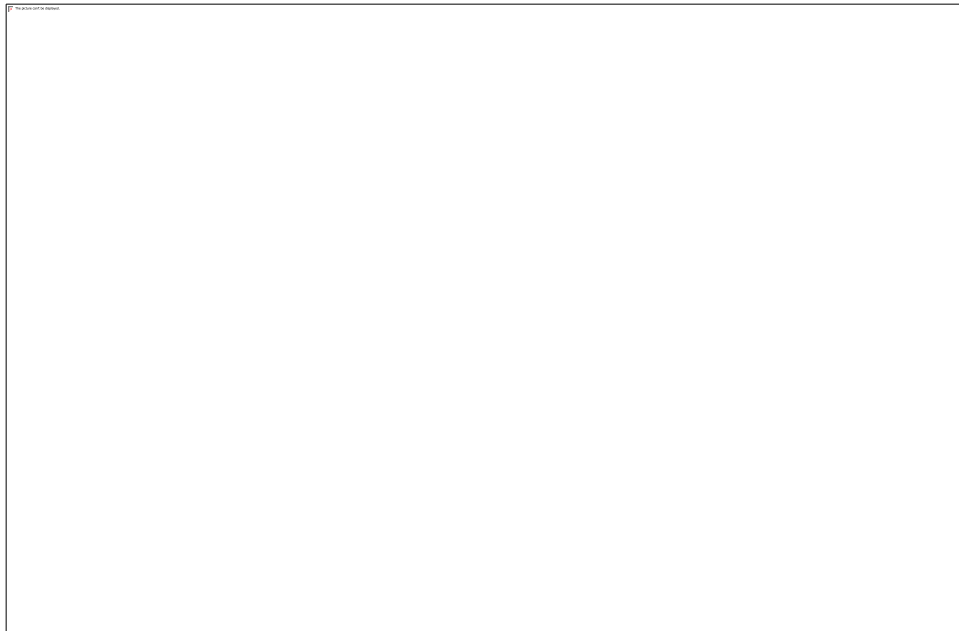
1. Place 7µL of cell suspension into one well of the hemocytometer, making sure the suspension is spreading beneath the glass slip.
2. Count all cells in the four corner sections (light colored squares below each consisting of 16 squares), as shown in Figure 1 and 2 above, under a 10X magnification.
3. Divide the total by 4 to obtain the average number of cells per square.
4. The volume of each square is 100nL (nano liters) or 1/10,000 ml. Calculate total count per mL using the formula below:
    a. Cells/mL Suspension = average # of cells per square X 10,000
5. Calculate the total number of cells in the pellet by multiplying the number of cells/mL suspension with the total volume of cell suspension from which the sample was drawn.
    a. Total number of cells in pellet = Cells/mL suspension X Total volume of suspension (in mL)
6. After calculating the total number of cells in the pellet, resuspend using an appropriate volume to reach the desired cell concentration for plating/other uses.

Appendix B: Protocol for Hanging Drop Spheroid Formation

Adapted from Professor Page at Worcester Polytechnic Institute

Purpose: To identify aggregation properties of various cell types.

Materials:

- Complete Cell Culture Media
- Sterile DPBS (-)
- Sterile tubes and culture plates/flasks
- Stereo Microscope
- Cells cultured to 70-80% confluency
- Incubator (5% CO2; 37°C)
- Biological Safety Cabinet (BSC)
- Serological pipets
- Motorized pipet aid
- Vacuum pump aspirator
- Sterilized Pasteur pipets
- Solvent resistant markers
- Spray bottle containing 70% ethanol
- Gloves

Procedure:

1. Complete the sub-culturing protocol outline in Appendix A.
2. Once a cell count and centrifugation are complete, resuspend cells to appropriate concentrations using complete media and a serological pipette.
   a. We resuspended for trials of 50K, 20K, 6 mil, and 12 mil in a 20µL drop.
3. In a new and sterile cell plate, add 7mL of DPBS (-) to maintain humidity during culture.
4. On the inside of the lid, pipette drops of the cell solution into rows in uniform drop sizes and shapes.
5. In a swift motion, replace the lid making sure that the cell drops do not get disturbed.
6. In the following days, observe the cell aggregations within the drops using a stereo microscope.

Appendix C: Protocol for Creation of Agarose Ring Molds

Adapted from Professor Rolle at Worcester Polytechnic Institute

Purpose: To create an agarose mold that promotes cell aggregation in a ring form.

Materials:

- Agarose Powder
- Digital scale
- Weigh boat and scoopula
- DMEM
- 24-well plate
- Pipette aid
- sterile pipettes of multiple sizes
- ring mold/punch
- Cells of choice at ~85% confluency
- Autoclave
- 50mL glass bottle
- BSC
- Microwave
- Hot plate

Procedure:

1. Transfer 50mL of DMEM to a 50mL bottle.
2. Weigh out 1g of agarose powder using a digital scale and add it to the 50mL bottle to create a 2% agarose solution.
3. Send solution to autoclave on the liquid cycle.
    a. Thorough mixing and sterilization will occur here.
4. When ready to create molds, move all supplies to BSC (24-well plate, pipettes, ring mold/punch)
5. Microwave 2% agarose solution with the cap slightly unscrewed for 2 minutes in 30 second increments, or until molten. The cap must be unscrewed slightly to release pressure build up in the bottle during heating. With a tight cap, there is risk of the bottle shattering during heating.
6. Quickly and carefully transfer the solution to the BSC and place on a hot plate set to medium to low heat for the agarose to remain molten. Adjust heat setting accordingly.
7. Pipette 1.6mL of molten agarose into the wells of a sterile 24-well plate. Fill as many wells to match how many punches are available for use at the time.
8. Before the solution solidifies, press the ring mold/punch into each well, careful not to reach the bottom of the well. Ensure that the solution fills in around the punch and avoid air bubbles and gaps.
9. Allow agarose solution to solidify around the ring mold/punch, and carefully remove the punch by pulling it straight up, but careful to not break off the newly formed agarose posts.
10. Once all ring well gels are formed, fill empty wells of the plate with DPBS (-), cover the plate, and place in the incubator for storage. The DPBS (-) and humidity of the incubator will limit evaporation from the gels to prevent the agarose from drying out while in storage.

Appendix D: Protocol for Creating Tissue Rings

Purpose: To create a 3D tissue ring from cells in a 2D culture.
Materials:
- 2% agarose ring molds in 24-well plate
- Cells in 2D culture
- Complete Cell Culture Media
- Incubator (5% CO2; 37°C)
- Biological Safety Cabinet (BSC)
- Micropipette and tips
- Serological pipets
- Motorized pipet aid
- Vacuum pump aspirator
- Sterilized Pasteur pipets
- Stereo microscope
- Solvent resistant markers
- Spray bottle containing 70% ethanol
- Gloves

Procedure:
1. Sub-culture the cells in 2D culture following the procedure in Appendix A.
2. Once a cell count and centrifugation are complete, resuspend cells to appropriate concentrations using complete media and a serological pipette.
   a. We resuspended for trials of 50K, 20K, 6M, and 12M in a 20μL drop.
3. With the agarose ring molds in the BSC, use the micropipette to carefully transfer the cell suspension into the ring wells of the agarose mold.
4. Place the plate in the incubator for at least 3-6 hours to allow for the cells to settle in the wells.
5. Once the cells settled, gently add 1mL of complete media along the side of each well and transfer the plate back into the incubator.
6. Image the cells within the following 4-6 days using a stereo microscope to ensure ring formation.

Appendix E: Protocol for Fibroblast and MDA-MB-231 Suspension Mixture Co-Culture

Purpose: To determine the efficacy of the *in vitro* tumor model in representing cancerous cell invasion in a scaffold less environment.

Materials:
- 2% agarose ring molds in 24-well plate
- HMF-52 cells in 2D culture
- MDA-MB-231 cells in 2D culture
- Media and media supplements
    - DMEM basal media with high glucose, sodium pyruvate, phenol red, sodium bicarbonate, Fetal bovine serum, Glutamax (200 mM), and Penn-Strep (100x)
- Incubator (5% CO2; 37°C)
- Biological Safety Cabinet (BSC)
- Micropipette and tips
- Serological pipets
- Motorized pipet aid
- Vacuum pump aspirator
- Sterilized Pasteur pipets
- Stereo microscope
- Fluorescent microscope
- Solvent resistant markers
- Spray bottle containing 70% ethanol
- Gloves

Procedure:
1. Sub-culture the HMF-52 cells in 2D culture following the procedure in Appendix A.
2. Once a cell count and centrifugation are complete, resuspend cells to appropriate concentrations using complete media and a serological pipette.
3. Create a suspension co-culture by adding a pre-determined number of MDA-MB-231 cells and HMF-52 cells into a new conical tube.
4. With the agarose ring molds in the BSC, use the micropipette to carefully transfer 10 µl of the HMF-52 and MDA-MB-231 cell suspension into the ring wells of the agarose mold.
5. Place the plate in the incubator for at least 3-6 hours to allow for the cells to settle in the wells.
6. Once the cells settled, gently add 1 mL of complete media along the side of each well and transfer the plate back into the incubator.
7. Image the cells within the following 4-6 days using a stereo microscope to ensure ring formation and monitor for cell invasion.
8. Once ring is formed, carefully remove tissue ring from mold, and image using a fluorescent microscope.

Appendix F: Protocol for Fibroblast and MDA-MB-231 Spheroid Co-Culture

Purpose: To determine the efficacy of the *in vitro* tumor model in representing cancerous cell invasion in a scaffold less environment.

Materials:
- 2% agarose ring molds in 24-well plate
- HMF-52 cells in 2D culture
- MDA-MB-231 cells in spheroids
- Media and media supplements
  - DMEM basal media with high glucose, sodium pyruvate, phenol red, sodium bicarbonate, Fetal bovine serum, Glutamax (200 mM), and Penn-Strep (100x)
- Incubator (5% CO2; 37°C)
- Biological Safety Cabinet (BSC)
- Micropipette and tips
- Serological pipets
- Motorized pipet aid
- Vacuum pump aspirator
- Sterilized Pasteur pipets
- Stereo microscope
- Fluorescent Microscope
- Solvent resistant markers
- Spray bottle containing 70% ethanol
- Gloves

Procedure:
1. Sub-culture the HMF-52 cells in 2D culture following the procedure in Appendix A.
2. Once a cell count and centrifugation are complete, resuspend cells to appropriate concentrations using complete media and a serological pipette.
3. With the agarose ring molds in the BSC, use the micropipette to carefully transfer 10 µl of the HMF-52 cell suspension into the ring wells of the agarose mold.
4. In each ring well with HMF-52 cells, transfer one MDA-MB-231 spheroid using a micropipette into the same well.
5. Place the plate in the incubator for at least 3-6 hours to allow for the cells to settle in the wells.
6. Once the cells settled, gently add 1 mL of complete media along the side of each well and transfer the plate back into the incubator.
7. Image the cells within the following 4-6 days using a stereo microscope to ensure ring formation and monitor for cell invasion.
8. Once ring is formed, carefully remove tissue ring from mold, and image using a fluorescent microscope.